

# **ADSORPTION BEHAVIOUR OF NITRIC OXIDE MOLECULES OVER Ni, Pd, AND Pt-EMBEDDED GRAPHITIC CARBON NITRIDE**

## **A Dissertation**

**Submitted to the Dean Office, Institute of Science and  
Technology, Tribhuvan University, Kirtipur in the Partial  
Fulfillment for the Requirements of Master's Degree of  
Science in Physics**



**By**

**Guna Nidhi Poudel**

**February, 2022**

# RECOMMENDATION



This is to certify that Mr. **Guna Nidhi Poudel** has carried out the Dissertation work entitled **“ADSORPTION BEHAVIOUR OF NITRIC OXIDE MOLECULES OVER Ni, Pd, AND Pt-EMBEDED GRAPHITIC CARBON NITRIDE”** under my advisory and guidance. I recommend the Dissertation in the partial fulfillment for the requirement of Master’s Degree of Science in Physics at Tribhuvan University.

*Rajendraparajuli*

(Supervisor)

Dr. Rajendra Parajuli

Professor

Amrit Campus, Tribhuvan University

Lainchour, Kathmandu

Date: *Feb 2, 2023*

## **ACKNOWLEDGEMENTS**

I would like to acknowledge the professional support, generosity, understanding, and consistent guidance that I received from my advisor, Prof. Dr. Rajendra Parajuli, for his guidance and instruction. His motivation, encouragement, observations, assistance, and comments have been very important throughout this work.

My sincere thanks go to Mr. Lok Bahadur Baral, Campus chief, Prof. Dr. Leela Pradhan Joshi, Head of the Department of Physics Amrit Campus, and Mr. Pitambar Shrestha, Coordinator of M.Sc. Program Amrit Campus for their invaluable suggestions, inspiration and for being supportive. I want to extend my gratitude to Dr. Hari Krishna Neupane for all of the suggestions, recommendations, and discussions. I would like to thank all the faculties and staff of the Department for their respective roles.

I would like to acknowledge University Grant Commission (UGC) for its partial financial support “The UGC masters research support 2077-2078” program.

I would like to acknowledge the International Science Program (ISP) for computer and VASP Software for our research program. And I am grateful to Prof. Dr. Shree Ram Sharma for coordinating the ISP and inspiring me to conduct research.

My research colleagues Anil Pudasaini, Dhan Raj Lawati, and Rupa Khanal deserve my gratitude. I gained a lot of knowledge from them. I would want to thank every one of my friends who have supported me in some way during this thesis study.

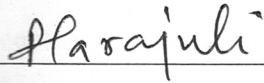
My heartfelt gratitude goes to my father and mother who supported me not only financially but also morally throughout my studies.

**Guna Nidhi Poudel**

## EVALUATION

This is to certify that we have evaluated this term paper entitled “**ADSORPTION BEHAVIOUR OF NITRIC OXIDE MOLECULES OVER Ni, Pd, AND Pt-Embedded GRAPHITIC CARBON NITRIDE**”, submitted by Mr. **Guna Nidhi Poudel** and in our opinion, it fulfills all the specified criteria, in the scope and quality, as a dissertation for the partial fulfillment of the requirement for the degree of Master of Science in Physics at Tribhuvan University.

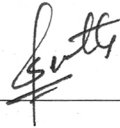
### Evaluation Committee



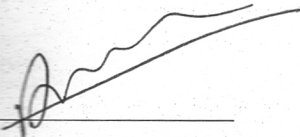
Prof. Dr. Rajendra Parajuli  
Supervisor  
Amrit Campus  
Tribhuvan University  
Lainchour, Kathmandu



Prof. Dr. Leela Pradhan Joshi  
Head, Department of Physics  
Amrit Campus  
Tribhuvan University  
Lainchour, Kathmandu



Pitambar Shrestha  
Coordinator, Department of Physics  
Amrit Campus  
Tribhuvan University  
Lainchour, Kathmandu



External Examiner



Internal Examiner

Date: Feb 17, 2023...

## ABSTRACT

Nitric Oxide adsorption on Ni, Pt, and Pd-Embedded graphitic carbon nitride has been studied computationally using density functional theory. PAW pseudopotential with PBE exchange-correlation functional in GGA approximation was used for the relax, SCF, electronics, and magnetic calculations. Kinetic energy cutoff 550 eV was set up for plane wave basis set with ‘Gaussian’ type smearing and width 0.05 eV. After relaxing, we get adsorbed energy of NO-GCN, NO-Ni-GCN, NO-Pd-GCN and NO-Pt-GCN are  $-1.68$  eV,  $-8.63$  eV,  $-6.61$  eV, and  $-8.74$  eV respectively. When functional transitional metals are embedded in GCN by adsorption of NO to its surface the results show that new energy states are introduced near the Fermi surface and modify the electronic properties of the system and the structure becomes a wrinkle. It means the conductivity of the system is considerably increased. Fermi energy of the GCN, NO adsorbs on GCN, NO adsorbs on Ni, Pd, Pt-Embedded GCN are  $-1.72$  eV,  $-1.36$  eV,  $-0.65$  eV,  $-0.64$  eV, and  $-0.61$  eV respectively. The band gap of the GCN, NO adsorbs on GCN, NO adsorbs on Ni, Pd, Pt-Embedded GCN are 1.3 eV, 1.12 eV, 0.98 eV, 0.45 eV and 0.32 eV respectively. During the adsorption process, electrons are transferred from the TM-Embedded GCN to NO molecules, due to metal the charge transfer from d-orbitals to the NO gas. So the bond length of NO in TM-Embedded GCN increases. The magnetic moment of these compounds is  $0 \mu_B$  except NO-Pt-GCN compound which has obtained  $0.98 \mu_B$  due to the  $d_{xy}$  and  $d_{yz}$  orbital of the Pt atom. The magnetic moment of Ni-GCN and Pd-GCN is found to be  $0 \mu_B$ .

# List of Figures

1.1	Structure of Graphitic Carbon Nitride (GCN) . . . . .	2
1.2	Nitric Oxide . . . . .	3
3.1	Electronic minimization flowchart (Internal algorithm of VASP) . . . . .	21
4.1	Geometrical structure of Nitric Oxide (a) Nitric Oxide before relax (b) Nitric Oxide after relax. . . . .	26
4.2	Unit cell of Graphitic Carbon Nitride . . . . .	27
4.3	Graphitic Carbon Nitride (a) Graphitic Carbon Nitride before relax (b) Graphitic Carbon Nitride after relax . . . . .	28
4.4	Band gap DOS plot of Graphitic Carbon Nitride. where $\Gamma$ - M- K- $\Gamma$ are high symmetry point, which is represented by a vertical dashed line. The horizontal dashed line represents Fermi level, which is set as 0 eV. . . . .	29
4.5	PDOS plot of C and N of Graphitic Carbon Nitride where fermi level set as zero . . . . .	29
4.6	Spin up and spin down DOS plot of GCN. Dashed lines indicates Fermi energy level which is set as 0 eV. . . . .	30
4.7	NO adsorbs Graphitic Carbon Nitride (a) side view NO adsorbs GCN before relax (b) top view NO adsorbs GCN before relax (c) top view NO adsorbs GCN after relax (d) side view NO adsorbs GCN after relax . . . . .	31
4.8	Band and DOS Plot of NO adsorbs Graphitic Carbon Nitride. where $\Gamma$ - M- K- $\Gamma$ are high symmetry point, which is represented by a vertical dashed line. The horizontal dashed line indicates the Fermi energy level, which is set as 0 eV . . . . .	32

4.9	Spin up and spin down plot NO adsorbs Graphitic Carbon Nitride. Dashed lines indicate Fermi energy level which is set as zero. . . . .	33
4.10	NO adsorbs Ni-Embedded Graphitic Carbon Nitride (a) side view of Ni-NO-gc3n4 before relaxed (b) top view of Ni-NO-gc3n4 before relaxed (c) side view of Ni-NO-gc3n4 after relaxed (d) top view of Ni-NO-gc3n4 after relaxed . . . . .	34
4.11	Band and DOS Plot of NO adsorbs Ni-Embedded Graphitic Carbon Nitride. where $\Gamma$ - M- K- $\Gamma$ are high symmetry point, which is represented by a vertical dashed line. The horizontal dashed line represents Fermi level, which is set as 0 eV. . . . .	35
4.12	(a) Magnetic Properties of Ni-Embedded Graphitic Carbon Nitride vertical dashed lines indicates Fermi energy level (b) Magnetic Properties of NO adsorbs Ni-Embedded Graphitic Carbon Nitride vertical dashed lines indicates Fermi energy level . . . . .	36
4.13	NO adsorbs Pd-Embedded Graphitic Carbon Nitride (a) side view of Pd-NO-GCN before relax (b) top view of Pd-NO-GCN before relax (c) side view of Pd-NO-GCN after relax (d) top view of Pd-NO-GCN after relax . . . . .	38
4.14	Electronic properties of NO adsorbs Pd-Embedded Graphitic Carbon Nitride. where $\Gamma$ - M- K- $\Gamma$ are high symmetry point, which is represented by a vertical dashed line. The horizontal dashed line represents Fermi level, which is set as 0 eV. . . . .	39
4.15	(a) Magnetic Properties of Pd-Embedded Graphitic Carbon Nitride. The vertical dashed line indicates Fermi energy level. (b) Magnetic Properties of NO adsorbs Pd-Embedded Graphitic Carbon Nitride. The vertical dashed line indicates Fermi energy level. . . . .	40
4.16	NO adsorbs Pt-Embedded Graphitic Carbon Nitride (a) side view of Pt-NO-GCN before relaxed (b) top view of Pt-NO-GCN before relaxed (c) side view of Pt-No-GCN after relaxed (d) top view of Pt-No-GCN after relaxed . . . . .	42
4.17	Electronic Properties of NO adsorbs Pt-Embedded Graphitic Carbon Nitride. Where $\Gamma$ - M- K- $\Gamma$ are high symmetry point, which is represented by a vertical dashed line. The horizontal dashed line represents Fermi level, which is set as 0 eV. . . . .	43
4.18	DOS of NO adsorbs Pt-Embedded GCN with spin up and spin down directions. . . . .	44

4.19	PDOS of NO adsorbs Pt-Embedded GCN with spin up and spin down directions.	
	(a)PDOS of N atom with spin up and spin down in NO adsorbs Pt embedded GCN.	
	(b)PDOS of C atom with spin up and spin down in NO adsorbs Pt embedded GCN.	45
4.20	DOS of NO adsorbs Pt-Embedded GCN with spin up and spin down directions.	
	(c)DOS of O atom with spin up and spin down in NO adsorbs Pt-Embedded GCN.	
	(d)DOS of Pt atom with spin up and spin down with $d_{xy}$ and $d_{yz}$ orbital in NO adsorbs Pt-Embedded GCN.	46



# List of Tables

1.1	Some physical parameters for the group VIII B elements. . . . .	4
4.1	Distance between two atoms in a monolayer of Graphitic Carbon Nitride . . . . .	27
5.1	Bond length . . . . .	54

## List of Abbreviations

<b>DFT</b>	Density functional theory
<b>GCN</b>	Graphitic carbon nitride
<b>NO</b>	Nitric Oxide
<b>Ni</b>	Nickel
<b>Pd</b>	Palladium
<b>PAW</b>	Projector augmented wave
<b>Pt</b>	Platinum
<b>SCF</b>	Self consistent field

# Contents

RECOMMENDATION . . . . .	i
ACKNOWLEDGEMENTS . . . . .	ii
EVALUATION . . . . .	iii
ABSTRACT . . . . .	iv
LIST OF FIGURES . . . . .	v
LIST OF TABLES . . . . .	vii
LIST OF ABBREVIATIONS . . . . .	ix
<b>1 Introduction</b>	<b>1</b>
1.1 Graphitic Carbon Nitride . . . . .	1
1.2 Nitric Oxide (NO) . . . . .	2
1.3 Transition Metals . . . . .	3
1.4 Literature Review . . . . .	4
1.5 Objectives of The Study . . . . .	5
1.6 Motivation . . . . .	6
<b>2 Theoretical Background</b>	<b>8</b>
2.1 General Consideration . . . . .	8
2.2 Many Body Schrödinger Wave Equation . . . . .	8
2.2.1 Born-Oppenheimer Approximation . . . . .	9
2.3 Single Particle Approximation . . . . .	10
2.3.1 Hartree Approximation . . . . .	10
2.3.2 Hartree-Fock Approximation . . . . .	11

2.4	Density Functional Theory (DFT)	13
2.4.1	Hohenberg Kohn Theorem	13
2.4.2	Kohn Sham Theorem	15
2.5	Exchange-Correlation Approximation	17
2.5.1	Local Density Approximation(LDA)	18
2.5.2	Generalized Gradient Approximation	18
2.6	Adsorption	19
<b>3</b>	<b>Research Methodologies</b>	<b>20</b>
3.1	VASP	20
3.2	PY4VASP	22
3.3	VESTA	23
3.4	VASPKIT	23
3.5	P4vasp	24
<b>4</b>	<b>Result and Discussion</b>	<b>25</b>
4.1	Geometry and Stability of Nitric Oxide	25
4.2	Graphitic Carbon Nitride	26
4.2.1	Single Graphitic Carbon Nitride	26
4.3	2 × 2 supercell of Graphitic Carbon Nitride	28
4.3.1	Electronic Properties of Graphitic Carbon Nitride	28
4.3.2	Magnetic Properties of Graphitic Carbon Nitride	30
4.4	NO adsorbs Graphitic Carbon Nitride	30
4.4.1	Electronic Properties of NO adsorbs Graphitic Carbon Nitride	32
4.4.2	Magnetic Properties of NO adsorbs Graphitic Carbon Nitride	32
4.5	NO adsorbs Ni-Embedded Graphitic Carbon Nitride	33
4.5.1	Electronic Properties of NO adsorbs Ni-Embedded Graphitic Carbon Nitride	34
4.5.2	Magnetic Properties of NO adsorbs Ni-Embedded Graphitic Carbon Nitride	35
4.6	NO adsorbs Pd-Embedded Graphitic Carbon Nitride	37

4.6.1	Electronic Properties of NO adsorbs Pd-Embedded Graphitic Carbon Nitride	38
4.6.2	Magnetic Properties of NO adsorbs Pd-Embedded Graphitic Carbon Nitride	39
4.7	NO adsorbs Pt-Embedded Graphitic Carbon Nitride . . . . .	41
4.7.1	Electronic properties of NO adsorbs Pt-Embedded Graphitic Carbon Nitride	42
4.7.2	Magnetic Properties of NO adsorbs Pt-Embedded Graphitic Carbon Nitride	43
<b>5</b>	<b>Conclusion and Future Prospects</b>	<b>47</b>
5.1	Conclusion . . . . .	47
5.2	Future Prospectus . . . . .	48
	<b>References</b>	<b>49</b>
	<b>Appendices</b>	<b>51</b>
	Appendix A . . . . .	51
A.1	Relax Calculation INCAR Input File . . . . .	51
A.2	SCF Calculation INCAR Input File . . . . .	52
A.3	DOS and Band Calculation INCAR Input File . . . . .	52
	Appendix B . . . . .	54
B.1	Bond Length . . . . .	54

# Chapter 1

## Introduction

Adsorption is the process by which a gas or liquid adheres to the surface of a solid. It is a surface phenomenon, meaning that it occurs at the interface between a gas or liquid and a solid. Such kind of adsorption can be either physical or chemical. Physical adsorption is a process in which the adhesion of a gas or liquid to a solid is caused by weak van der Waals forces between the molecules of the gas or liquid and the surface of the solid. Chemical adsorption, on the other hand, occurs when the gas or liquid molecules interact with the surface of the solid through chemical bonds. Adsorption is an important process in many different fields, including chemistry, materials science, and engineering. For example, adsorption is used in the purification of gases and liquids, in the production of materials such as activated carbon and zeolites, and in the design of devices such as gas masks and air filters [1].

### 1.1 Graphitic Carbon Nitride

Graphitic Carbon Nitride (GCN) is a two-dimensional, layered material composed of carbon and nitrogen atoms. Sheets of Graphitic Carbon Nitride are made up of C and N atoms with  $sp^2$  hybridization. The bond of partial N atoms are connected with two neighbors C atom is unsaturated. The 2D structure of graphitic carbon nitride is analogous to the graphite (i.e. weak van der Waals interaction between two adjacent layers and strong covalent bonding interconnection in plane atoms). There are five phases in  $C_3N_4$ , which are  $\alpha - C_3N_4$ ,  $\beta - C_3N_4$ , cubic  $-C_3N_4$ , pseudocubic  $-C_3N_4$

and GCN. Among them, GCN has a narrow bandgap and good light absorption. There are two types of structure, tri-s-triazine ( $C_6N_7$ ) or triazine ( $C_3N_3$ ), in which tri-s-triazine is the stable structure. In this structure, rings are connected in a triangular shape which is closely seen as graphene layers [2].

Among various materials, Graphitic Carbon Nitride (g- $C_3N_4$  or GCN) has significantly attracted the attention of its good characteristics such as environmental friendliness, low preparation cost, suitable band gap energy, high surface area for adsorption, and excellent physicochemical stability. GCN is stable up to 600 °C. At recent years, Graphitic Carbon Nitride(GCN) nanosheets have remarkable interest due to their adsorption behaviour, catalysis and photocatalysis. GCN is the stable structure, therefore it is expected that the space between the triazine group is the important center for the trapping of the cations, transitional metal, and the adsorbed molecule with large radii inside it [3].

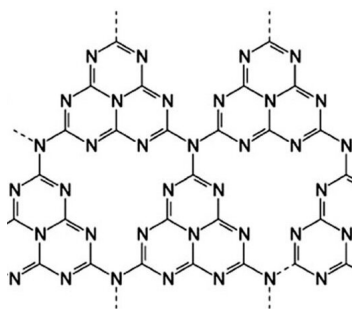


**Figure 1.1.** Structure of Graphitic Carbon Nitride (GCN)

## 1.2 Nitric Oxide (NO)

Nitric Oxide is a colorless gas with the formula NO. It is one of the principal oxides of nitrogen. An intermediate in industrial chemistry, Nitric Oxide forms a combustion system, and can be generated by lightning in thunderstorms. In mammals, including humans, nitric oxide is a signaling molecule in many physiological and pathological processes.



**Figure 1.2.** Nitric Oxide

However, Nitric Oxide is a major gas pollutant, which is extremely hazardous to the environment such as acid rain, and ozone layer depletion. NO gas is the byproduct of fossil fuel plants, and automobile and industrial factories. In recent years NO gas is significantly increasing in the air over the past few decades.

### 1.3 Transition Metals

Transition elements are elements found on the periodic table in Groups 3-12. The term refers to the fact that the d sublevel that is being filled is at a lower principal energy level than the s sublevel that came before it. An atom with an oxidation number of -1 accepts an electron to achieve a more stable configuration. The electron donation is then +1. When a transition metal loses electrons, it usually loses s orbital electrons first, followed by d orbital electrons.

Most transition metals have multiple oxidation states because transition metals lose electron(s) more easily than alkali metals and alkaline earth metals. The valence s-orbital of alkali metals contains one electron, and their ions almost always have oxidation states of +1 (from losing a single electron). Similarly, alkaline earth metals have two electrons in their valence s-orbitals, resulting in +2 oxidation state ions (from losing both). Transition metals, on the other hand, are more complex and exhibit a variety of observable oxidation states, owing primarily to the removal of d-orbital electrons [4].



**Table 1.1.** Some physical parameters for the group VIII B elements.

Element	Electronic configuration	Melting Point(K)	Boiling Point(K)	Density(gm/cm <sup>3</sup> )
Ni	[Ar] 3d <sup>8</sup> 4s <sup>2</sup>	1728.00	3003	8.908
Pd	[Kr]4d <sup>10</sup>	1828.05	3236	12.023
Pt	[Xe]4f <sup>14</sup> 5d <sup>9</sup> 6s <sup>1</sup>	2041.40	4098	21.450

## 1.4 Literature Review

There are a variety of research works in the field of Graphitic Carbon Nitride. Basharnavaz et al. (2018) studied the Ni, Pd, and Pt-Embedded Graphitic Carbon Nitride as excellent adsorbents for HCN removal: A DFT study. In this research, they found that Pt-Embedded GCN has more adsorption energy (−1.98 eV) than other embedded Graphitic Carbon Nitride. And they concluded that Pt-Embedded GCN displayed the highest affinity for the adsorption of HCN among the proposed adsorbents [5].

Basharnavaz et al. (2019) studied the interaction of CO molecules with VIII transition metals-Embedded Graphitic Carbon Nitride as an excellent candidate for CO sensor. The result of the work is that spin-polarized band structure of pristine GCN, Ni and Pd-Embedded systems are non-magnetic, whereas Pt-Embedded gCN induces non-zero magnetic moment equal to 1.35  $\mu$ B. And they also concluded that Pt-Embedded gCn is more effective than those of the other adsorbents in sensing and removing the gas from the atmosphere [6].

Again, Basharnavaz et al. (2019) studied that Fe, Ru, and Os-Embedded Graphitic Carbon Nitride as a promising candidate for NO gas sensors. In this research, they show that among Fe, Ru, and Os-Embedded GCN systems, the Os-Embedded GCN has the best adsorption [7].

Ghosh et al. (2014) studied the magnetism and optical properties of transition metal embedded Graphitic Carbon Nitride sheet. They studied various transition metals and found that V, Cr, and Fe-Embedded GCN interact ferromagnetically with each other, and results in a ferromagnetic ground state. However, Mn couples antiferromagnetically, and Cu and Zn are non-magnetic in the ground state of their corresponding TM-GCN [8].

Aspera et al. (2010) studied the adsorption of water on tri-s-triazine-based Graphitic Carbon Nitride which obtain an adsorption energy is 0.82eV with a barrier energy of 0.02eV. In this study, the most stable configuration would be on top of the two-coordinate nitrogen atom in an orientation where one O-H bond is parallel to the surface and the other one is pointing to surface [9].

Hu et al. (2020) studied the electronic and magnetic properties of embedded transitional metal in GCN monolayer. They studied adsorption behavior by using ligand field theory and Hund's rule and obtain magnetic behavior with various transitional metals. The system remains semiconducting but reduced band gap by the adsorption of Cr or Ni atoms and by the adsorption of V and Co atom semiconducting Graphitic Carbon Nitride change into magnetic metal [10].

xu et al. (2020) studied the adsorption behavior of HCN, SO<sub>2</sub>, H<sub>2</sub>S, and NO molecules on Graphitic Carbon Nitride with embedded Mo atom. They found that the adsorption of HCN, SO<sub>2</sub>, and H<sub>2</sub>S makes the system semimetal properties, while NO produces a smaller magnetic moment. According to the charge transfer analysis HCN, SO<sub>2</sub> and NO acts as acceptors, while H<sub>2</sub>S acts as a donor [11].

Wu et al. (2015) studied the role of the defect on the adsorption of water on Graphitic Carbon Nitride. From this study water monomer, dimer, and cluster with three and four molecules can form a stable adsorption structure being coplanar with GCN sheet. The suitable structures are water dimer and cluster. Water dissociates at the defect site and finally, it forms a mixed adsorption structure with hydrogen, hydroxyl and water molecules at the defect site. The defects in GCN monolayer play an important role in the adsorption and dissociation of water [12].

Aspera et al. (2017) studied the molecular interaction of O<sub>2</sub> with tri-s-triazine-based GCN. From this study, O<sub>2</sub> molecule adsorbed physically on the surface of GCN through the interactions of the lowest unoccupied molecular orbital with two nitrogen with the surface. These results would be important for the intermediate surface oxidation step in nitrogen and carbon-based catalyst [13].

## 1.5 Objectives of The Study

The general objective of our research work is:

- To study the adsorption behavior of Nitric Oxide with the Ni-Embedded, Pd-Embedded, and Pt-Embedded GCN

The specific objectives of our research work are:

- To study the adsorption energy of Nitric Oxide with GCN, Ni-Embedded, Pd-Embedded, and Pt-Embedded GCN
- To study the structural properties of Nitric Oxide with GCN, Ni-Embedded, Pd-Embedded, and Pt-Embedded GCN
- To study the electronic properties of Nitric Oxide with GCN, Ni-Embedded, Pd-Embedded, and Pt-Embedded GCN
- To study the magnetic properties of Nitric Oxide with GCN, Ni-Embedded, Pd-Embedded, and Pt-Embedded GCN.

## **1.6 Motivation**

The study of the adsorption behavior of Nitric Oxide (NO) on different forms of Graphitic Carbon Nitride (GCN) is an important research area in the field of material science and environmental engineering. Nitric Oxide is a key air pollutant that contributes to the formation of smog and acid rain, and it is also a major contributor to greenhouse gas emissions. The adsorption of NO on different forms of GCN can potentially be used for the removal of NO from the atmosphere, making it an important area of research.

Previous research has shown that transition metal-Embedded GCN, such as Ni, Pd, and Pt-Embedded GCN, have excellent adsorption properties for various gases, including HCN and CO. For example, Basharnavaz et al. (2018) found that Pt-Embedded GCN has the highest adsorption energy for HCN among the proposed adsorbents. Similarly, Basharnavaz et al. (2019) found that Pt-Embedded GCN is more effective than other adsorbents in sensing and removing CO from the atmosphere.

The use of density functional theory (DFT) calculations in previous research has been a valuable tool in understanding the adsorption behavior of gases on GCN. DFT calculations have been used

to study the adsorption energy, structural properties, electronic properties, and magnetic properties of gases on GCN. These calculations have been used to predict the adsorption behavior of gases on GCN and to understand the underlying mechanism of adsorption.

Given the importance of NO in air pollution and the potential of GCN as an adsorbent, the study of the adsorption behavior of NO on Ni, Pd, and Pt-Embedded GCN using DFT calculations is an important and timely research area. This thesis aims to study the adsorption behavior of NO on GCN, Ni-Embedded GCN, Pd-Embedded GCN, and Pt-Embedded GCN using DFT calculations. By studying the adsorption energy, structural properties, electronic properties, and magnetic properties of NO on these different forms of GCN, this research aims to contribute to the understanding of the adsorption behavior of NO on GCN and to the development of GCN-based adsorbents for the removal of NO from the atmosphere.

# Chapter 2

## Theoretical Background

### 2.1 General Consideration

In this section, we will discuss the theoretical background involved in the calculation of our systems. All systems are composed of mutually interacting electrons and nuclei and the dynamics of these particles. In general, all systems are composed of mutually interacting electrons and nuclei. V. Fock's approach assumes that each electron in the system moves under the combined average field of the nucleus and other electrons. This is an approximation for calculating the wave function and energy of a stationary quantum multi-particle system. The antisymmetric nature of the wave functions is accurately taken into consideration. This approach works for atoms, molecules, nanostructures, and solids for solving the Schrodinger equation.

### 2.2 Many Body Schrödinger Wave Equation

All system which are mutually interacting with electrons-electrons, electrons-nuclei and nuclei-nuclei. Many body Schrödinger wave equation solve these problems by considering wave function

$$\Psi_{total} = \Psi(r_1^{\vec{}}, r_2^{\vec{}}, r_3^{\vec{}}, \dots, r_N^{\vec{}}, t)$$

The most common form of many body Schrödinger equation is

$$\hat{H}\Psi_{total} = E\Psi_{total}$$

There are several approximation to solve the many body Schrödinger wave equation but we discuss Born-Oppenheimer approximation.

### 2.2.1 Born-Oppenheimer Approximation

In 1927, two scientist Max Born and J. Robert Oppenheimer derived the Born-Oppenheimer approximation. This approximation is based on that the motion of electrons and nucleus can be separated in the molecules. Total Wavefunction can be separated into the electronic and nuclear component.

$$\Psi_{total} = \Psi_{electronic} \times \Psi_{nucleus}$$

Neglecting the relativistic spin orbit interaction between electron and nucleus then total Hamiltonian can be written as

$$\hat{H} = \sum_{I=1}^N \frac{\hat{P}_I^2}{2M_I} + \sum_{i=1}^{N_e} \frac{\hat{P}_i^2}{2m} + \sum_{i>j} \frac{e^2}{|\vec{r}_i - \vec{r}_j|} + \sum_{I>J} \frac{Z_I Z_J e^2}{|\vec{R}_I - \vec{R}_J|} - \sum_{i,I} \frac{Z_I e^2}{|\vec{R}_I - \vec{r}_i|} \quad (2.1)$$

$$= T_N + T_e + V_{ee}(\vec{r}) + V_{NN}(\vec{R}) + V_{Ne}(\vec{r}, \vec{R}) \quad (2.2)$$

Where, R denotes the nuclear coordinates and r denotes electronic coordinates.

Because  $\frac{M}{m} \gg 10^3$ , one can regard the nuclei as fixed for the motion of electrons. So, kinetic energy of the nucleus acts as a small perturbation term. By applying this approximation we can neglect the kinetic energy of the nucleus then 2.2.1 becomes

$$\hat{H}_0 = \sum_{i=1}^{N_e} \frac{\hat{P}_i^2}{2m} + \sum_{i>j} \frac{e^2}{|\vec{r}_i - \vec{r}_j|} - \sum_{i,I} \frac{Z_I e^2}{|\vec{R}_I - \vec{r}_i|} \quad (2.3)$$

Therefore, the Schrödinger equation for the electronic motion can be written as

$$(\hat{H}_0 + V_{NN})\Psi_{electronic} = E_{elec}\Psi_{electronic} \quad (2.4)$$

The Schrödinger equation for the nuclear motion can be written as

$$(T_N + E_{elec})\Psi_{nucleus} = E\Psi_{nucleus} \quad (2.5)$$

For vibrational electronic spectra, rotational fine structure we use nuclear wavefunction and For band gap, density of states etc. we use electronic wavefunction [14].

## 2.3 Single Particle Approximation

The exact Hamiltonian for the solid and introducing approximations in its solution, which lead to sets of single-particle equations for the electronic degrees of freedom in the external potential created by the presence of the ions. Each electron experiences the presence of other electrons through an effective potential in the single-particle equations. This effective potential encapsulates the many-body nature of the true system in an approximate way [15].

### 2.3.1 Hartree Approximation

Schrödinger equation is given by

$$\left[ \sum_i \{H_i^0 + V_i(r_i)\} \right] \Psi(r_1, r_2, r_3, \dots, r_N) = E\Psi(r_1, r_2, r_3, \dots, r_N) \quad (2.6)$$

where,  $H_i^0 = \left( \frac{P_i^2}{2\mu} \right) - \left( \frac{Ze^2}{r_i} \right)$

$$V_i(r_i) = \sum_{i < j} \int |u_j(r_j)|^2 \frac{e^2}{r_{ij}} d^3r_j = \text{Hartree field} \quad (2.7)$$

The eigenfunction  $\Psi(r_1, r_2, r_3, \dots, r_N)$  are called atomic orbitals.

$V_i(r_i)$  is a one electron operator. Therefore, regarding  $\Psi$  as a simple product of one-electron wave functions, i.e.

$$\Psi(r_1, r_2, r_3, \dots, r_N) = u_1(r_1)u_2(r_2)\dots u_N(r_N) \quad (2.8)$$

Therefore, Schrödinger equation can be separated into  $N$  equations of the form

$$\left[ H_i^0 + V_i(r_i) \right] u_i(r_i) = E_i u_i(r_i) \quad (2.9)$$

General solution of one electron function is,

$$u_i = R(r_i)Y(\theta, \phi) \quad (2.10)$$

Where,  $u_i$  are called the central field orbitals so only radial part is involves for unknown potential  $V_i(r_i)$ . To solve the Schrödinger equation Hartee used the method Successive approximation. In the

zeroth approximation he used hydrogen like wave functions  $u_j^0$ , which give

$$V_i^0(r_i) = \sum_{i < j} \int |u_j^0(r_j)|^2 \frac{e^2}{r_{ij}} d^3r_j \quad (2.11)$$

Use these  $V_i^0(r_i)$  to obtain  $u_i^1$  in the first approximation

$$\left[ H_i^0 + V_i^0(r_i) \right] u_i^1(r_i) = E_i^0 u_i^1(r_i) \quad (2.12)$$

The solutions  $u_i^1$  of this set of equations give a new potential energy

$$V_i^1 = \sum_{i < j} \int |u_j^1|^2 \frac{e^2}{r_{ij}} d^3r_j \quad (2.13)$$

This process continued until one arrives at

$$V_i^H = \sum_{i < j} \int |u_j^H|^2 \frac{e^2}{r_{ij}} d^3r_j \quad (2.14)$$

Which when put in the equation

$$\left[ H_i^0 + V_i^H \right] u_i^H(r_i) = E_i^H u_i^H \quad (2.15)$$

The potential energy  $V_i^H$  is called *Self consistent Hartree field*.

Hartree doesn't include the motion of electrons caused by the asymmetry of complete wavefunction He doesn't include exchange term in energy. Therefore Hartree method gives same energy for the ortho and para states of Helium [16].

### 2.3.2 Hartree-Fock Approximation

For a system of two electrons,

$$H = H_1^0 + H_2^0 + V_{12}$$

Where,  $H_1^0$  = the Hamilton of the electron 1

$H_2^0$  = the Hamilton of the electron 2

The Slater determinant for the ground state is,

$$\Psi = \frac{1}{\sqrt{2}} \begin{vmatrix} u_a(1) & u_b(1) \\ u_a(2) & u_b(2) \end{vmatrix}$$



where,  $\langle u_a|u_a\rangle = 1$ ,  $\langle u_b|u_b\rangle = 1$  (normalization)

$\langle u_a|u_b\rangle = \langle u_b|u_a\rangle = 0$  (orthogonality)

Which ensures that the Pauli principle is satisfied.

$$\langle \Psi|H|\Psi\rangle = \langle u_a|H^0|u_a\rangle + \langle u_b|H^0|u_b\rangle + \langle u_a(1)u_b(2)|V_{12}|u_a(1)u_b(2)\rangle - \langle u_a(1)u_b(2)|V_{12}|u_b(1)u_a(2)\rangle$$

Solving above equation by using Lagrange's multipliers then obtain,

$$H_1^0 u_a(1) + \left[ \sum_{j \neq i} \int u_j^*(2) \left( \frac{e^2}{r_{12}} \right) u_j(2) d^3 r_2 \right] u_i(1) - \sum_{j \neq i} \left[ \int u_j^*(2) \left( \frac{e^2}{r_{12}} \right) u_i(2) d^3 r_2 \right] u_j(1) = E_i u_i(1)$$

$$\left[ H_1^0 + \sum_j \left[ J_j(1) - K_j(1) \right] \right] u_i(1) = E_i u_i(1)$$

Where,

$$J_j(1) = \int u_j^*(2) \left( \frac{e^2}{r_{12}} \right) u_j(2) d^3 r_2 = \text{Coulomb Operator}$$

$$K_j(1) = \int u_j^*(2) \left( \frac{e^2}{r_{12}} \right) u_i(2) d^3 r_2 = \text{Exchange Operator}$$

$$F(1) = H_1^0 + V(1) = \text{Fock Operator}$$

$$V(1) = \sum_j \left[ J_j(1) - K_j(1) \right]$$

So eigenvalue equation

$$F(1)u_i = E_i u_i(1) \quad (2.16)$$

Separating space and spin parts and then,

$$J_j(1) = \int \phi_j^*(2) \left( \frac{e^2}{r_{12}} \right) \phi_j(2) d^3 r_2 = \text{Coulomb term}$$

$$K_j(1) = \delta(m_s^i, m_s^j) \int \phi_j^*(2) \left( \frac{e^2}{r_{12}} \right) \phi_i(2) d^3 r_2 = \text{Exchange term}$$

In Hartree Fock method the interaction of one electron with the another electron is treated with the mean-field approximation, which neglects the instantaneous interactions of the electrons. Electrons repel with each other, therefore the position of one electron affects the position of another electron. And also if one electron is on one side of the molecule, the other electron is likely to be on the other side. This effect is not included in a Hartree-Fock calculation. Such kind of affect is called correlation affect, which is solve by the density functional theory [16].

## 2.4 Density Functional Theory (DFT)

The solutions obtained by the Hartree-Fock method are not very accurate. The DFT approach solved this difficulty by calculating the system's total energy in terms of its energy density. This approach is used to study the electronic structure of many-body systems, specifically atoms, and molecules, as well as the condensed phase. Functionals that are spatially dependent on electron density can be used to estimate the parameters of many-electron systems (i.e. electron density functionals). Ab initio methods, semiempirical methods, the density functional method, and the molecular mechanics method are the four basic approaches to computing molecular characteristics. The Hohenberg-Kohn theorem and the Kohn-Sham technique demonstrated that the interacting system's energy may be calculated in terms of electron density.

### 2.4.1 Hohenberg Kohn Theorem

For a system of  $N$  electrons, Pierre Hohenberg and Walter Kohn established the immensely practical and conceptual significance of density-functional theory in 1964. They demonstrated that the ground-state molecular energy, wave function, and all other molecular electronic properties are all governed by the ground-state electron probability density  $\rho_0(x, y, z)$  for molecules with a nondegenerate ground state

**Theorem I.** "For any system of interacting particles in an external potential  $V_{ext}(\vec{r})$ , the potential  $V_{ext}(\vec{r})$  is uniquely determined, except for constant, by the ground-state particle density  $n_0(\vec{r})$ ."

Let us consider  $\Psi$  is the ground state wavefunction and  $H$  is the Hamiltonian of the system, then ground state energy is written as,

$$E = \langle \Psi | H | \Psi \rangle = \langle T \rangle + \langle V_{ext} \rangle + \int d^3r V_{ext}(\vec{r}) n(\vec{r}) \quad (2.17)$$

Suppose there are two different external potentials  $V_{ext}^{(1)}(\vec{r})$  and  $V_{ext}^{(2)}(\vec{r})$  which differ more than a constant and that lead to the same ground state-density  $n(\vec{r})$ . The two external potentials give two Hamiltonians,  $\hat{H}_1$  and  $\hat{H}_2$ , which have different ground state wavefunctions  $\Psi^{(1)}$  and  $\Psi^{(2)}$ . Since

$\Psi^{(2)}$  is not the ground state of  $\hat{H}_1$ , it follows that

$$E^1 = \langle \Psi^{(1)} | \hat{H}_1 | \Psi^{(1)} \rangle < \langle \Psi^{(2)} | \hat{H}_1 | \Psi^{(2)} \rangle \quad (2.18)$$

The inequality follows if the ground state is nondegenerate. The last term of Eq. 2.18 can be written as

$$\langle \Psi^{(2)} | \hat{H}_1 | \Psi^{(2)} \rangle = \langle \Psi^{(2)} | \hat{H}_2 | \Psi^{(2)} \rangle + \langle \Psi^{(2)} | \hat{H}_1 - \hat{H}_2 | \Psi^{(2)} \rangle \quad (2.19)$$

$$= E^2 + \int d^3r \left[ V_{ext}^{(2)}(\vec{r}) - V_{ext}^{(1)}(\vec{r}) \right] n_0(\vec{r}) \quad (2.20)$$

So,

$$E^1 < E^2 + \int d^3r \left[ V_{ext}^{(1)}(\vec{r}) - V_{ext}^{(2)}(\vec{r}) \right] n_0(\vec{r}) \quad (2.21)$$

On the other hand if we consider  $E^2$  in same way, we find the same equation with superscripts (1) and (2) interchanged,

$$E^2 < E^1 + \int d^3r \left[ V_{ext}^{(2)}(\vec{r}) - V_{ext}^{(1)}(\vec{r}) \right] n_0(\vec{r}) \quad (2.22)$$

Now we add Eqs. 2.21 and 2.22 we get contradictory inequality

$$E^{(1)} + E^{(2)} < E^{(2)} + E^{(1)} \quad (2.23)$$

This shows that there cannot be two different external potentials differing by more than a constant that give rise to the same nondegenerate ground state charge density. The density is uniquely determines the external potential within a constant.

**Theorem II.** Hohenberg Kohn Theorem II The density that minimizes the total energy is the exact ground state density.

According to this theorem, If electron density  $n(r)$  determines  $V_{ext}(\vec{r})$  then  $N$  and  $V_{ext}(\vec{r})$  determines  $\hat{H}$  and therefore  $\Psi$ . Then expectation value of  $\hat{F}$  is also a functional of  $n(\vec{r})$ .

$$F[n(\vec{r})] = \langle \Psi | \hat{F} | \Psi \rangle \quad (2.24)$$

Where,  $V$  is representation of energy function  $F[n(r)]$  at which  $V_{ext}(\vec{r})$  is unrelated to another density  $n'(\vec{r})$

$$E_G[n'(\vec{r})] = \int n'(\vec{r})V_{ext}(\vec{r})dr + F[n'(\vec{r})] \quad (2.25)$$

Now,

From variational principle

$$\langle \Psi' | \hat{F} | \Psi' \rangle + \langle \Psi' | \hat{V}_{ext} | \Psi' \rangle > \langle \Psi | \hat{F} | \Psi \rangle + \langle \Psi | \hat{V}_{ext} | \Psi \rangle \quad (2.26)$$

If  $\Psi$  is wave function with correct ground state ground state  $n(\vec{r}) \approx n_0(\vec{r})$  then

$$\int n'(\vec{r})V_{ext}(\vec{r})dr + F[n'(\vec{r})] > \int n(\vec{r})V_{ext}(\vec{r})dr + F[n(\vec{r})] \quad (2.27)$$

$$E_G[n'(\vec{r})] > E_G[n_0(\vec{r})] \quad (2.28)$$

This indicates that energy functional  $E_G[n_0(\vec{r})]$  whose existence is unique; is minimal of the exact ground state density and its minimum gives the exact ground state energy of many body electron system [17].

## 2.4.2 Kohn Sham Theorem

Kohn Sham equation are obtained by minimizing the Hohenberg Kohn theorem.

Energy functional  $E[n(\vec{r})]$  is related to external potential as,

$$E[n(\vec{r})] = F[n(\vec{r})] + \int n(\vec{r})V_{ext}(\vec{r})dr \quad (2.29)$$

where,  $F[n(\vec{r})] = T[n(\vec{r})] + V_{ee}[n(\vec{r})]$  is universal i.e. doesn't depend on  $V_{ext}$ . Here,  $E[n(\vec{r})]$  is unknown and need to be appropriately approximated by K-S theorem.

To carryout this, the variational approach is used to ground state density  $n(\vec{r})$  of interacting electron system is decomposed into sum of N-independent orbitals contribution of the form.

$$n(\vec{r}) = \sum_i \Phi_i^*(\vec{r})\Phi_i(\vec{r}) \quad (2.30)$$

Where,  $\Phi_i(\vec{r})$  are orbitals.

If  $\Phi_i(\vec{r}); [i = 1, 2, 3 \dots N]$  denote N-orbitals of lowest energy of the system on non-interacting electron. Ground state wavefunction is just Slater determinant and electron density will be

$$n_0(\vec{r}) = \sum_i \Phi_i^*(\vec{r})\Phi_i(\vec{r})$$

Since,  $n_0(\vec{r}) = n(\vec{r})$  is, decomposition 2.30 is satisfied.

Similarly, for interacting electrons ground states of interacting electron system do not form Slater determinant with orbitals contributing to  $n(\vec{r})$

Adding kinetic energy functional of the non-interacting system  $T_s[n]$  to both sides of equation 2.29, we get

$$E[n(\vec{r})] + T_s[n] = F[n(\vec{r})] + T_s[n] + \int n(r)V_{ext}(r)dr$$

$$E[n(\vec{r})] = T_s[n] + \{T[n] - T_s[n] + v[n]\} + \int n(r)V_{ext}(r)dr \quad (2.31)$$

Again Hartree term on both sides of equation 2.31, we get

$$E[n] = T_s[n] + \left\{ T[n] - T_s[n] + V[n] - \frac{e^2}{2} \int \int \frac{n(r)n(r')}{|r-r'|} dr dr' \right\} + \frac{e^2}{2} \int \int \frac{n(r)n(r')}{|r-r'|} dr dr' + \int n(r)V_{ext}(r)dr \quad (2.32)$$

let  $E_{xc}[n] = \left\{ T[n] - T_s[n] + V[n] - \frac{e^2}{2} \int \int \frac{n(r)n(r')}{|r-r'|} dr dr' \right\}$  Then,

$$E[n] = T_s[n] + E_{xc}[n] + \frac{e^2}{2} \int \int \frac{n(r)n(r')}{|r-r'|} dr dr' + \int n(r)V_{ext}(r)dr \quad (2.33)$$

Thus, exchange correlation energy function is,

$$E_{xc}[n] = \left\{ T[n] - T_s[n] + V[n] - \frac{e^2}{2} \int \int \frac{n(r)n(r')}{|r-r'|} dr dr' \right\}$$

$$E_{xc}[n] = F_{HK}[n] - \frac{e^2}{2} \int \int \frac{n(r)n(r')}{|r-r'|} dr dr' - T_s[n]$$

Where,  $F_{HK} = T[n] + V[n]$

Now develop reasonable approximations for  $E_{xc}[n]$

To minimize the functional  $E_{xc}[n]$  with respect to  $n$ . We use variation of 2.33 with respect to particle density,

$$\frac{\delta E[n]}{\delta n(\vec{r})} = \frac{\delta T_s[n]}{\delta n(\vec{r})} + \frac{\delta E_{xc}[n]}{\delta n(\vec{r})} + e^2 \int \frac{n(\vec{r}') dr'}{|r - r'|} + V_{ext}(\vec{r})$$

$$\frac{\delta E[n]}{\delta n(\vec{r})} = \frac{\delta T_s[n]}{\delta n(\vec{r})} + V_{xc}[n] + e^2 \int \frac{n(\vec{r}') dr'}{|r - r'|} + V_{ext}(\vec{r}) \quad (2.34)$$

where,  $V_{xc}[n] = \frac{\delta E_{xc}[n]}{\delta n(\vec{r})}$

$$\frac{\delta T_s[n]}{\delta n(\vec{r})} + V_{ks}(\vec{r}) = 0 \quad (2.35)$$

Where,  $V_{ks}(\vec{r}) = V_{ext}(\vec{r}) + V_{xc}(\vec{r}) + V_{coulomb}(\vec{r})$  Now, using variational principle of the energy functional of 2.33 leads to Kohn-Sham equation as,

$$\left[ -\frac{\hbar^2}{2m} + V_{ks} \right] \Phi_i(\vec{r}) = E_i \Phi_i(\vec{r}) \quad (2.36)$$

Once Kohn-Sham orbitals and energies have been determined the exact ground state energy and all terms can be calculated easily with reasonable guess of Exchange correlation function  $E_{xc}[n]$  [18].

## 2.5 Exchange-Correlation Approximation

The exchange-correlation approximation deals with the exchange correlation function which can be done with varying degree depending upon the approach taken. But in general the functional can be written as

$$E_{xc}[n(\vec{r})] = \int n(\vec{r}) E_{xc}(\vec{r}) dr \quad (2.37)$$

The functional 2.37 can be characterized by the way in which the density surrounding each electron is sampled in order to construct  $E_{xc}(\vec{r})$

### 2.5.1 Local Density Approximation(LDA)

The simplest approximation of which is applied to a uniform (homogeneous) electron gas. Let the exchange-correlation energy per particle be  $E_{xc}$ , then from the K-S theorem the exchange-correlation function LDA can be approximated as 2.37 Here in LDA, density of the system varies very slowly. So that the exchange correlation energy i.e. locally that of a homogeneous system at local density. The exchange correlation potential produced by functional will given by

$$V_{xc}^{LDA} = \frac{\delta E_{xc}^{LDA}[n(r)]}{\delta n(r)}$$

$$V_{xc}^{LDA} \approx E_{xc}[n(r)] + n(r) \frac{dE_{xc}[n(r)]}{dn(r)}$$

In LDA, the total ground state energy  $E_0^{LDA}$  can be written as [18],

$$E_0^{LDA} = \sum_i E_i - \frac{1}{2} \int n(r) \frac{e^2}{|r-r'|} n(r') dr dr' - \int n(r) \frac{dE_{xc}(n)}{dn(r)} dr + E_{xc}[n]$$

### 2.5.2 Generalized Gradient Approximation

When calculating the energy, we always try to correlate the theoretical and experimental results. So, we use exchange-correlation which is the correction of kinetic energy and potential energy. Exchange correlation is dependent only on the electron density distribution. In this approximation energy of the exchange-correlation is the function of electron density and density gradient. The local density assumes that the density is everywhere. Because of this local density approximation(LDA) has a tendency to underestimate the exchange energy and overestimate correlation energy. Nowadays exchange-correlation energy functions that utilize both the electron density and its gradient or slope (first derivatives with respect to position). These functional are called generalized gradient approximation (GGA). The exchange-correlation energy functional can be written as the sum of an exchange-energy functional and a correlation-energy functional, both negative, i.e.  $E_{XC} = E_X + E_C$ ;  $E_X$  is much bigger than  $E_C$  in magnitude. We write probability density( $\rho$ ) as:

$$\rho = |\psi(\vec{r}, t)|^2 \quad (2.38)$$

Then exchange-correlation energy can be written as:

$$E_{xc}^{GGA} = E_{xc}[\rho(\vec{r}), \nabla\rho(\vec{r})] \quad (2.39)$$

And then exchange correlation potential can be written as:

$$V_{xc} = \frac{\partial E_{xc}}{\partial \rho(\vec{r})} \quad (2.40)$$

By this equation, we can calculate the exchange correlation potential [19].

## 2.6 Adsorption

When a solid surface is exposed to a gas or a liquid, molecules from the gas or the solution phase accumulate at the surface. The phenomenon of accumulation of molecules of a gas or liquid at a solid surface is called adsorption. The substance that accumulates at the surface is called Adsorbate and the solid on whose surface the accumulation occurs is called the Adsorbent. There are two types of adsorption.

1. physisorption

A reversible phenomenon that is a result of the intermolecular force of attraction between molecules of adsorbent and adsorbate. This is due to the non-local electronic interactions, named van der Waals forces [20].

2. chemisorption

An irreversible phenomenon that is a result of bond formation between atoms of adsorbent and adsorbate. This is due to the local electronic rearrangement.

Adsorption phenomena are exothermic, in order to balance the unbalanced forces of the surface molecule. Adsorption is a surface phenomenon, the extent of adsorption depends on the surface area. Increase the surface of the adsorbent, and increase the total amount of gas adsorbed.

For our research adsorption energy is calculated as [1]:

$$E_{ads} = E_{gCN-NO} - E_{gCN} - E_{NO}$$

Where,

$E_{gCN-NO}$ =Total energy of gCN with NO gas,

$E_{NO}$ =Energy of isolated NO,

$E_{gCN}$ =Energy of isolated gCN.



# Chapter 3

## Research Methodologies

### 3.1 VASP

VASP stands for Vienna Ab initio Simulation Package. This package is used for performing ab initio quantum mechanical calculations. The features of VASP are as follows:

- Structural relaxation by using conjugate gradient methods
- Molecular dynamics by using Born-Oppenheimer molecular dynamics
- Phonons, elastic constants (including ionic contributions), internal strain tensors
- Forces and stress tensor for DFT, Hartree-Fock, and hybrid functionals
- Many-body perturbation theory
- Fly machine learning force fields
- Calculation of magnetism and linear responses to the electric field.

In VASP calculation, the electronic charge density, the one-electron orbitals, and the local potential are expressed in plane wave basis sets. It computes the solution of the many-body Schrödinger equation by solving either density functional theory (by using Kohn-Sham equations), or Hartree-Fock (HF) approximation (by using the Roothaan equations). Additionally, Hybrid functionals are also used that combine the Hartree-Fock strategy with density functional theory[21].

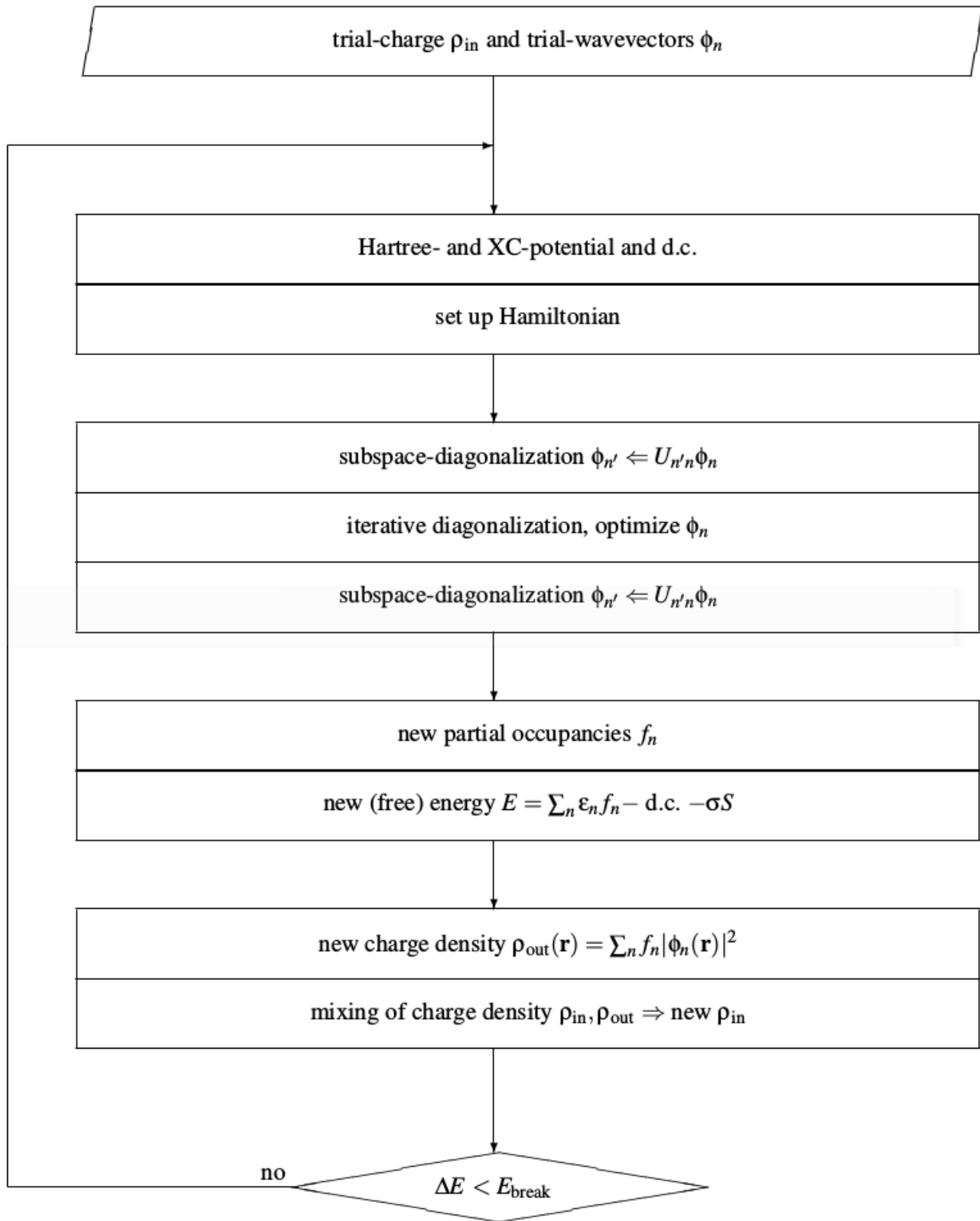


**Figure 3.1.** Electronic minimization flowchart (Internal algorithm of VASP)

[22]

The algorithm used by VASP is an iterative matrix-diagonalization scheme, where the used algorithms are based on the conjugate gradient scheme, block Davidson scheme, and residual minimization scheme - direct inversion in the iterative subspace (RMM-DIIS).

### **Input file description**

POSCAR = It contains lattice geometry and ionic positions used in the calculation.

POTCAR = It contains the pseudopotential of each atomic species used in the calculation.

KPOINTS = It contains k points.

INCAR = It contains the algorithms and set the parameters that VASP uses during the calculation.

To run this input file we use the following command in the command prompt:

```
./vasp_std
```

After this, the calculation is running. The following output file is seen in the current folder.

### **Output file description**

CHG = It contains the lattice vectors, atomic coordinates, and the total charge density multiplied by the volume.

CHGCAR = It contains charge density and the PAW one-center occupancies.

CONTCAR = It contains the relaxed lattice geometry and ionic positions.

DOSCAR = It contains the DOS and integrated DOS.

EIGENVAL = It contains the Kohn-Sham-eigenvalues for all k-points.

IBZKPT = It contains the k-point coordinates.

OSZICAR = It contains convergence speed, about the current step, energy, and change in energy.

PCDAT = It contains the pair correlation function.

OUTCAR = It contains a summary of the used input parameters, stress tensors, forces on the atoms, local charges and magnetic moments, dielectric properties.

## **3.2 PY4VASP**

A Python interface called py4vasp is used to extract data from VASP calculations. Its primary goals are to provide a fast overview of the data and the ability to export it into common formats for use by other, more advanced postprocessing programs. People who want to create Python scripts based

on the data collected by VASP fall under the second application domain. This program eliminates parsing problems caused by the XML or OUTCAR files by interacting directly with the new HDF5 file format [23].

It is used for the band, DOS, dielectric function, and dielectric tensor plot. It is a fast tool to plot data obtain from the VASP calculation without extracting data from it.

### **3.3 VESTA**

VESTA is open-source software for 3D visualization programs for crystal morphologies, structural models, and volumetric data such as electron/nuclear densities. It read \*.vest, \*.vasp, \*.cif, \*.xtl, \*.p1, \*.XSF etc. extension file. The software allows you to deal with a virtually unlimited number of objects such as atoms, bonds polyhedra, and polygons on isosurfaces in multiple windows, each of which may contain multiple tabs corresponding to files. VESTA enables you to visualize interatomic distances and bond angles that are restrained in Rietveld analysis with RIETAN-FP and supports lattice transformation from conventional to non-conventional lattice by using matrices. Other features include the ability to run arithmetic operations among multiple volumetric data files and to export high-resolution graphic images which incorporate smooth rendering of isosurfaces and sections. It determines the best plane for selected atoms and displaying the labels of atoms [24].

The main purpose of this software for this work is as follows:

- To visualize the molecular structure, and arranged the atom in the proper position with the help of GUI
- Construct the structure of the molecule and set the position of the atom with visualized.
- To prepare the input file for the VASP i.e. POSCAR file.

### **3.4 VASPKIT**

VASPKIT uses Fortran 90 programming language. It provides a powerful and user-friendly interface to perform various material properties from the raw data calculated by the VASP. It has mainly

two modules such as pre-processing modules and post-processing modules.

In pre-processing modules, it manipulates input data such as input file generation, symmetry analysis, supercell transformation, and band path generation for a given crystal structure. In the post-processing module, it extracts and analyzes the raw calculated data about elastic mechanics, electronic structure, charge/spin density, electrostatic potential, and linear optical coefficients [25].

### **3.5 P4vasp**

P4VASP is a powerful and open-source 3D visualization tool for the VASP molecular dynamics and computational chemistry software package.

P4Vasp is one of the Graphical User Interfaces to visualize spacial arrangements of atoms from their geometrical coordinates. Using directly the output files generated by the first principle modeling package VASP, this software is rather popular [26].

# Chapter 4

## Result and Discussion

The transitional metals Ni, Pd, and Pt embedded in GCN by the adsorption of NO to its surface were investigated computationally. Self-consistent, electronic, and magnetic computations were performed using the Projector Augmented Wave (PAW) pseudopotential and Perdew-Burke-Ernzerhof (PBE) exchange-correlation functional in the Generalized Gradient Approximation (GGA). NO firstly optimized to get the relaxed structure and optimized GCN with K points grid  $5 \times 5 \times 1$ . After relaxing the structure, SCF calculation was performed for GCN, NO adsorbs GCN, NO adsorbs Ni embedded GCN, NO adsorbs Pd embedded GCN and NO adsorbs Pt embedded GCN. After full structural optimization, large vacuum space more than 17 Å along the lattice vector (c vector or z direction) was set to avoid any interaction between sheet. Tetrahedron method was used to compute the band gap.  $25 \times 25 \times 1$  K points grid was selected in order to get the band gap. VASPKIT was used for generating K grid points, whereas  $\Gamma$ - M- K-  $\Gamma$  are the high-symmetry points. In the INCAR file, ISPIN=2 gives information about the magnetic moment.

### 4.1 Geometry and Stability of Nitric Oxide

In this research, we used Nitric Oxide as the adsorbent molecule. Nitric Oxide is a free radical that has an unpaired electron. fig. 4.1 shows the before- and after-relax structures of Nitric Oxide.

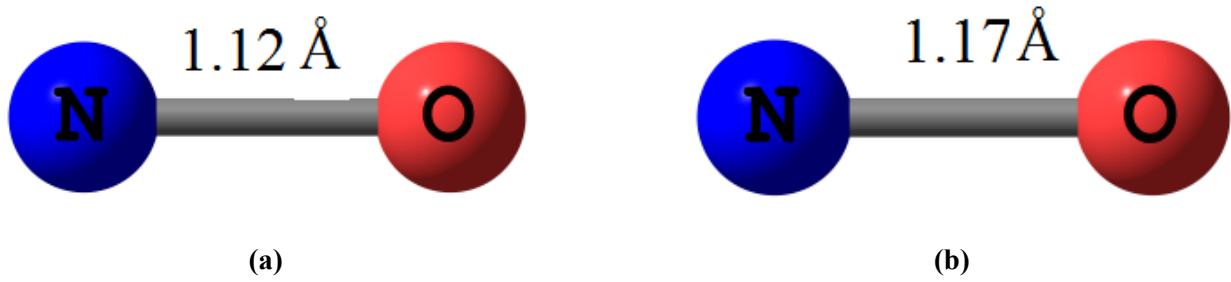


**Figure 4.1.** Geometrical structure of Nitric Oxide (a) Nitric Oxide before relax (b) Nitric Oxide after relax.

Initially, the distance between nitrogen and oxygen was given by  $1.12 \text{ \AA}$  and after relaxation, the distance became  $1.17 \text{ \AA}$ . The relaxing energy of Nitric Oxide is found to be  $-12.03 \text{ eV}$ ; this is consistent with the previous result [27].

## 4.2 Graphitic Carbon Nitride

### 4.2.1 Single Graphitic Carbon Nitride

Graphitic Carbon Nitride is made up of carbon and nitrogen with a triangular shape. In the monolayer, there are 14 atoms ( 8 nitrogen atoms and 6 carbon atoms). The calculated lattice constant for this unit cell is found to be  $7.1 \text{ \AA}$  which is consistent with [28] previous results. Table 4.1 shows the distance between each atom (Carbon and Nitrogen) after relaxation. Based on the optimized structure, it can be found that all of the C-N bond lengths in this unit cell are  $1.33 \text{ \AA}$ , except for the  $C_{inner}-N_{inner}$  ( $1.39 \text{ \AA}$ ) and  $C_{bridge}-N_{bridge}$  ( $1.49 \text{ \AA}$ ), which are in excellent agreement with the previous reports [9],[13].

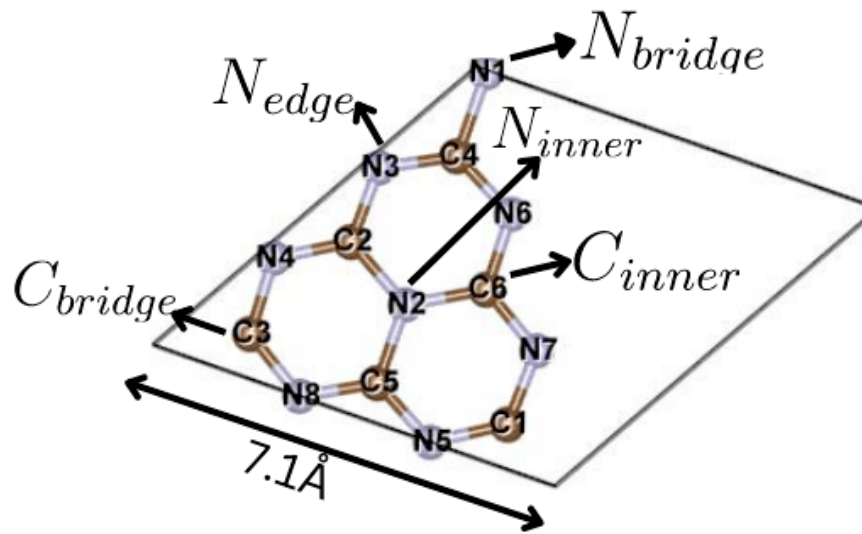


**Figure 4.2.** Unit cell of Graphitic Carbon Nitride

**Table 4.1.** Distance between two atoms in a monolayer of Graphitic Carbon Nitride

Atoms	Bonds length(Å)	
	Before Relax	After Relax
N1-C4	1.48	1.49
N3-C4	1.32	1.33
N3-C2	1.33	1.33
N4-C2	1.32	1.33
N4-C3	1.33	1.33
N8-C5	1.32	1.33
N5-C5	1.33	1.33
N5-C1	1.33	1.33
C1-N7	1.32	1.33
N7-C6	1.33	1.33
C6-N6	1.32	1.33
C5-N2	1.37	1.39
C6-N2	1.38	1.39
C2-N2	1.40	1.39



### 4.3 $2 \times 2$ supercell of Graphitic Carbon Nitride

In  $2 \times 2$  supercell, there are vacancies between 4 unit cells where different atoms and molecules can be embedded. From the relax calculation, the relaxed structure is obtained which is shown in fig. 4.3. The relax distance of this supercell are given in Appendix B. The Relax energy of this system was found to be  $-472.17434$  eV.

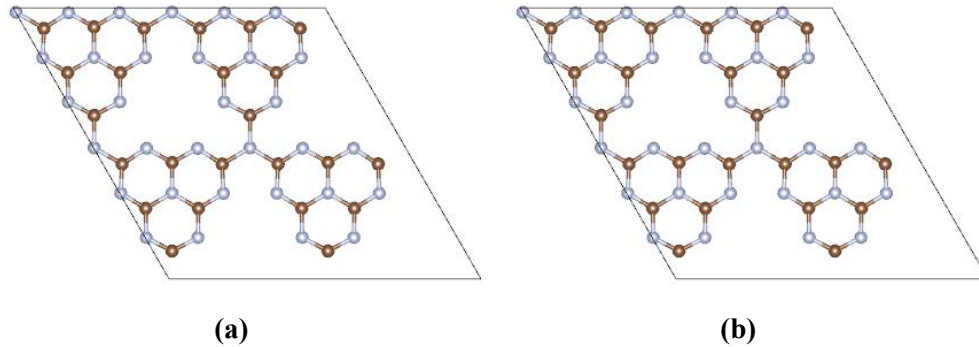


**Figure 4.3.** Graphitic Carbon Nitride (a) Graphitic Carbon Nitride before relax (b) Graphitic Carbon Nitride after relax

#### 4.3.1 Electronic Properties of Graphitic Carbon Nitride

Figure. 4.4 shows the band and DOS plot of Graphitic Carbon Nitride. The Fermi energy of this system is found to be  $-1.72$  eV which is comparable with the previous results [6], [11], [28] and [29]. Horizontal dashed lines indicates the Fermi energy level, which set as 0 eV. From this calculation, band gap of GCN was found to be 1.3 eV.

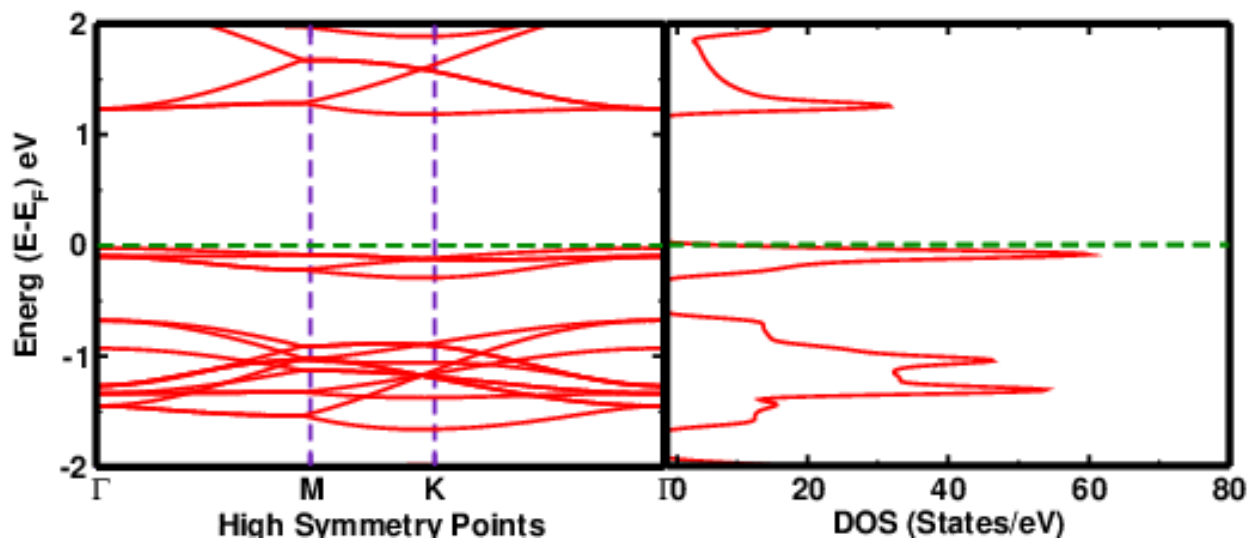


**Figure 4.4.** Band gap DOS plot of Graphitic Carbon Nitride. where  $\Gamma$ - M- K- $\Gamma$  are high symmetry point, which is represented by a vertical dashed line. The horizontal dashed line represents Fermi level, which is set as 0 eV.

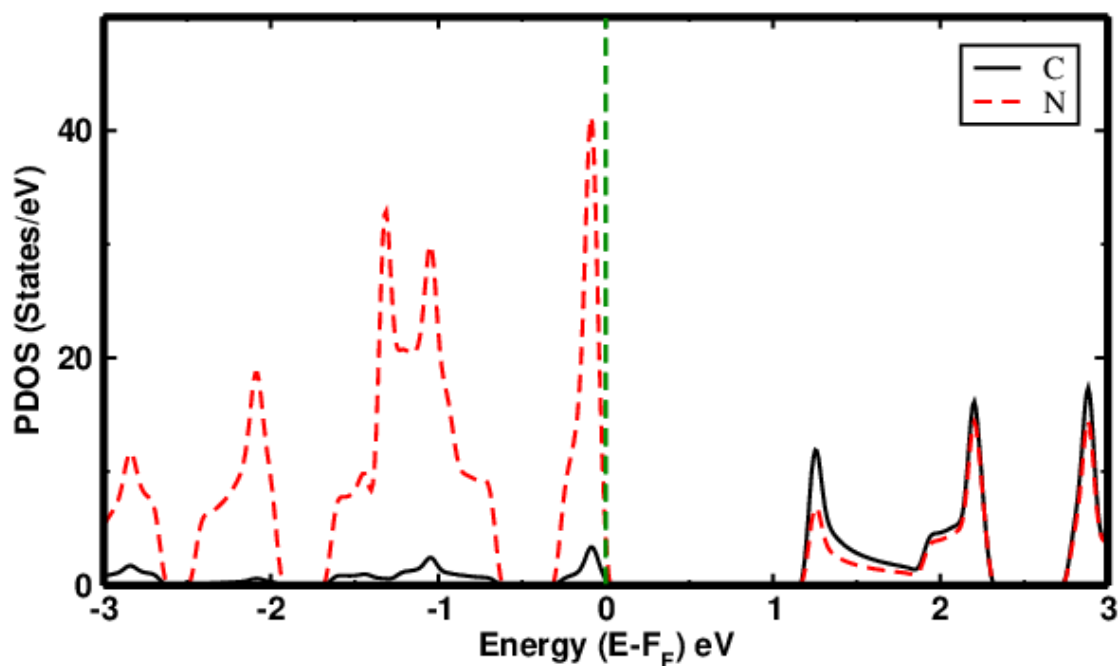


**Figure 4.5.** PDOS plot of C and N of Graphitic Carbon Nitride where fermi level set as zero

Figure. 4.5 represents the PDOS plot of GCN. This diagram shows that nitrogen plays a significant role in the valence band and carbon plays an important role in the conduction band.

### 4.3.2 Magnetic Properties of Graphitic Carbon Nitride

In Figure 4.6 upper lines indicate DOS of spin up and below lines indicate DOS of spin down of the GCN, Carefully observing this figure own can see that there are symmetry between spin up and spin down. Symmetry between spin up and spin down doesn't give magnetic nature of the material. Magnetic moment of this material is found to be  $0.0 \mu_B$ . That means GCN is not magnetic material.

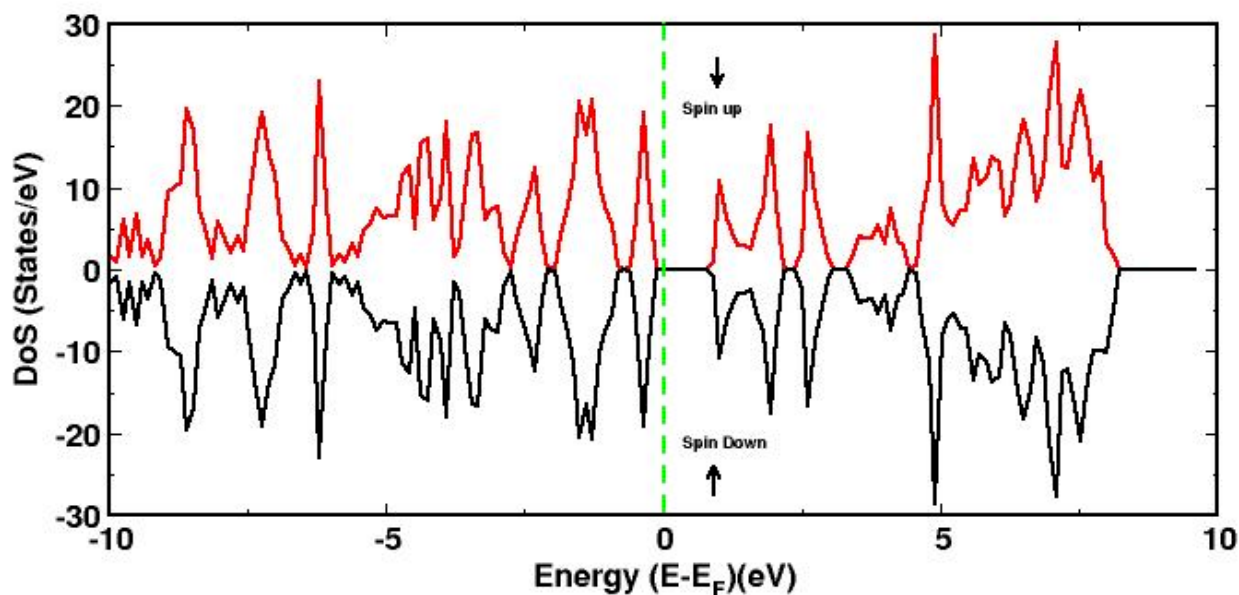


**Figure 4.6.** Spin up and spin down DOS plot of GCN. Dashed lines indicates Fermi energy level which is set as 0 eV.

## 4.4 NO adsorbs Graphitic Carbon Nitride

After relaxing  $2 \times 2$  Graphitic Carbon Nitride, Nitric Oxide is adsorbed on it. The initial side view of NO adsorbed GCN is depicted in fig 4.7a, the same top view structure of this system is given in fig 4.7b. The same relaxed structure is given in fig 4.7c and 4.7d respectively. After relaxation, the distance between nitrogen and oxygen is found to be  $1.17 \text{ \AA}$ . Initially, this distance was found to be  $1.17 \text{ \AA}$  in Nitric Oxide. That means, there is no change in the distance between Nitrogen and Oxygen. Additionally, Nitric Oxide is rotated at an angle and moved from its initial position. Relaxation energy of the Nitric Oxide adsorbs GCN was found to be  $-485.8865 \text{ eV}$ . Adsorption energy is calculated by the formula 2.6 and it is found to be  $-1.68 \text{ eV}$ . Moreover, it can be found

that with adsorption of NO gas over GCN, the initial flat structure of pristine GCN automatically becomes wrinkle, because the buckle structure of GCN is more stable than the flat one, which is in agreement with the previous results [7]. Here, physisorption of Nitric Oxide with GCN occurs.

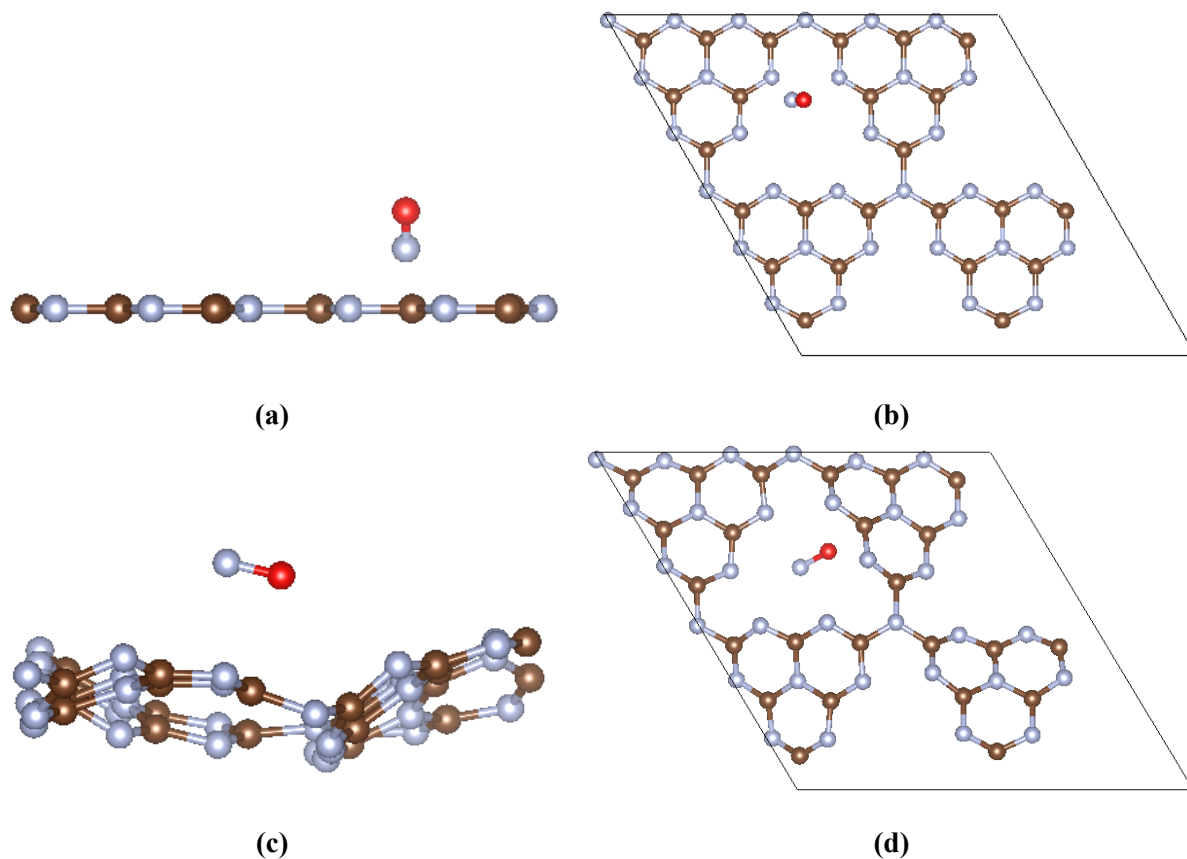


**Figure 4.7.** NO adsorbs Graphitic Carbon Nitride (a) side view NO adsorbs GCN before relax (b) top view NO adsorbs GCN before relax (c) top view NO adsorbs GCN after relax (d) side view NO adsorbs GCN after relax

#### 4.4.1 Electronic Properties of NO adsorbs Graphitic Carbon Nitride

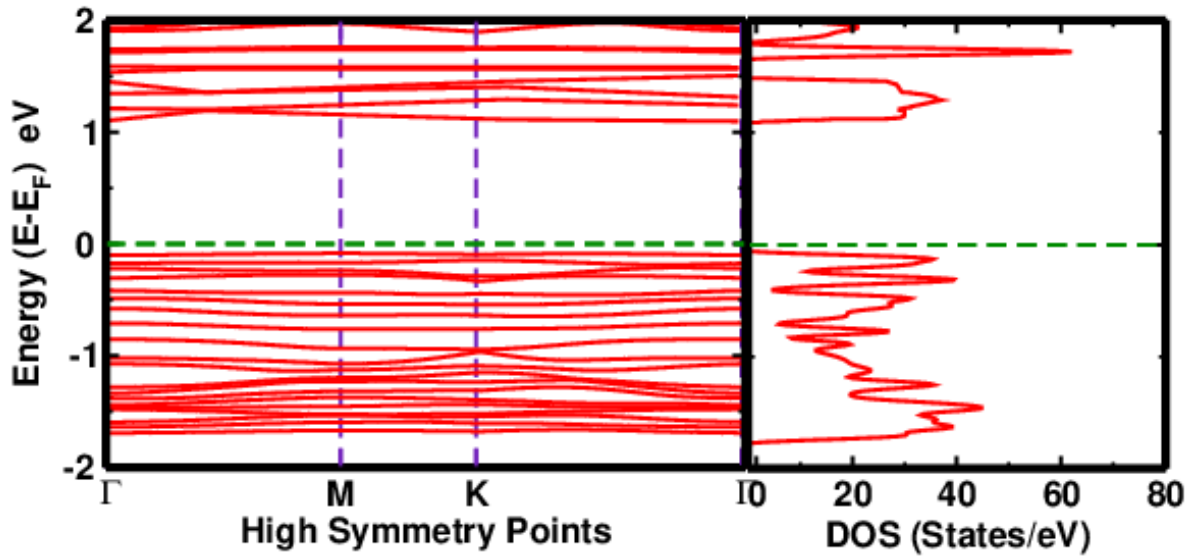


**Figure 4.8.** Band and DOS Plot of NO adsorbs Graphitic Carbon Nitride. where  $\Gamma$ - M- K- $\Gamma$  are high symmetry point, which is represented by a vertical dashed line. The horizontal dashed line indicates the Fermi energy level, which is set as 0 eV

Figure 4.8 shows the band and DOS plot of NO adsorbs GCN. In this calculation, the Fermi energy of NO-GCN is found to be  $-1.36$  eV which is smaller than the GCN Fermi energy. The horizontal dashed line indicates the Fermi level, which is set as 0 eV. The band gap energy of NO adsorbs GCN is found to be 1.12 eV, which is in agreement with the previous reports [27].

#### 4.4.2 Magnetic Properties of NO adsorbs Graphitic Carbon Nitride

In Figure 4.9, upper lines indicate DOS of spin up, and below lines indicate DOS of spin-down of the NO adsorbs GCN. Carefully observing this figure we can see that there is symmetry between spin up and spin down. The symmetry between spin up and spin down doesn't give the magnetic nature of the material. The magnetic moment of this material is found to be  $0.0 \mu_B$ . That means NO adsorbs GCN is not magnetic material.

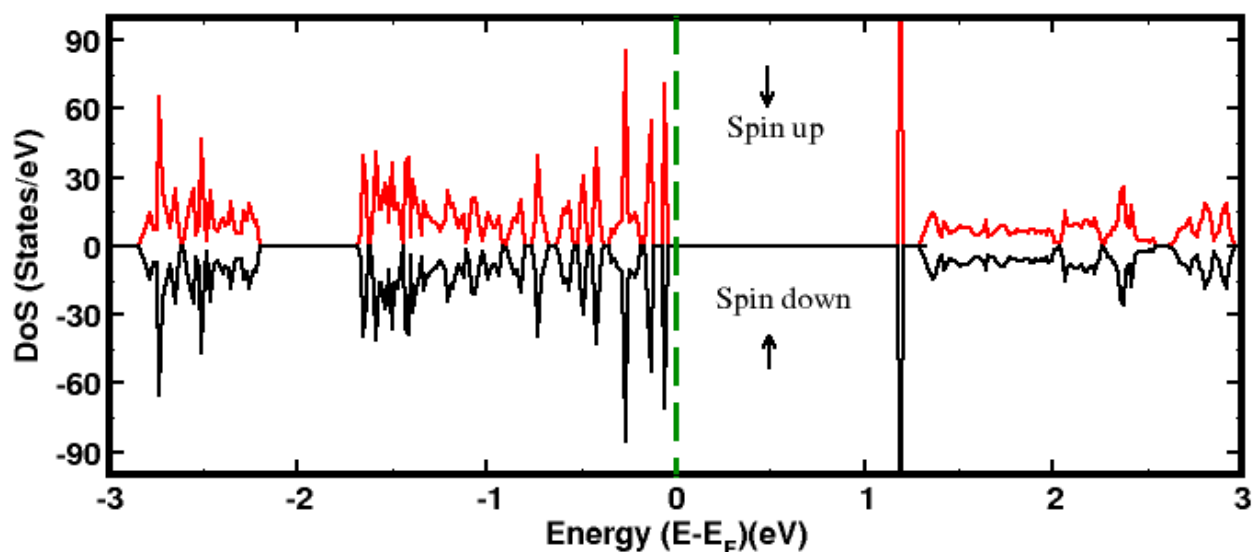


**Figure 4.9.** Spin up and spin down plot NO adsorbs Graphitic Carbon Nitride. Dashed lines indicate Fermi energy level which is set as zero.

## 4.5 NO adsorbs Ni-Embedded Graphitic Carbon Nitride

Ni is the transition metal that is embedded on the Graphitic Carbon Nitride. Simultaneously Nitric Oxide adsorbs on this Ni-Embedded Graphitic Carbon Nitride. Fig 4.10a (side view) and Fig4.10b (top view) are the structure of NO adsorbs Ni-Embedded Graphitic Carbon Nitride before relaxation. The same relaxed structure is given in Fig 4.10c (side view) and Fig 4.10d (top view) respectively. Moreover, it can be found that with the adsorption of NO gas over Ni-Embedded GCN, the initial flat structure of pristine GCN automatically becomes wrinkle, because the buckle structure of GCN is more stable than the flat one, which is in agreement with the previous results [7]. Distance between respected atoms in 4.10 is given in Appendix B. When comparing bond length with GCN and NO-GCN, the outside side of the bond length is about 2 Å longer whereas the inner side is unaffected.

The distance between nitrogen and oxygen in Nitric Oxide after relaxation was found to be 1.173 Å. Relaxation energy of the Nitric Oxide adsorbs Ni embedded GCN was found to be  $-493.05$  eV. Adsorption energy is calculated by the formula 2.6 and it is found to be  $-8.63$  eV. Here, chemisorption of Nitric Oxide with Ni-Embedded GCN occurs. Nitric Oxide forms the bond with the Nickel

with bond length 1.62 Å, Which is smaller than Pd-NO and Pt-NO.

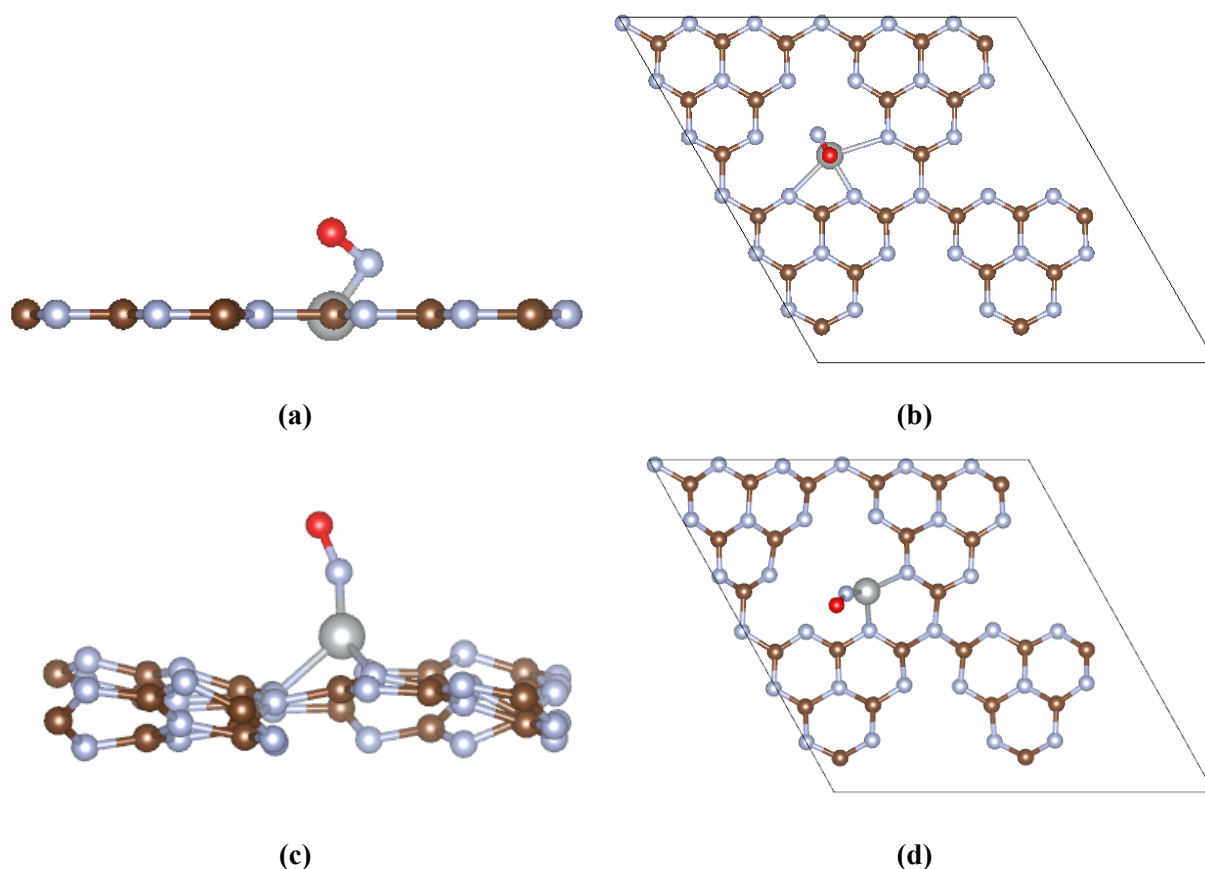


**Figure 4.10.** NO adsorbs Ni-Embedded Graphitic Carbon Nitride (a) side view of Ni-NO-gc3n4 before relaxed (b) top view of Ni-NO-gc3n4 before relaxed (c) side view of Ni-NO-gc3n4 after relaxed (d) top view of Ni-NO-gc3n4 after relaxed

#### 4.5.1 Electronic Properties of NO adsorbs Ni-Embedded Graphitic Carbon Nitride

Figure. 4.11 shows the DOS plot of NO adsorbs Ni-Embedded Graphitic Carbon Nitride. In this calculation, the Fermi energy of NO adsorbs Ni-GCN is found to be  $-0.66$  eV which is comparable with the previous reports [6], [11], [29] and [28]. The results show that Ni-Embedded Graphitic Carbon Nitride with Nitric Oxide adsorbs, new energy states are introduced near the Fermi surface and modify the electronic properties of the system. It means the conductivity of the system is considerably increased. In figure 4.11 some bands are added nearly on the Fermi surface so, the

band gap of Ni-Embedded GCN becomes 0.98 eV. DOS is shifted towards the Fermi level, and the highest density of states is obtained at energy level nearly  $-2$  eV (valence band), which is nearly equal to the 70 States/eV.

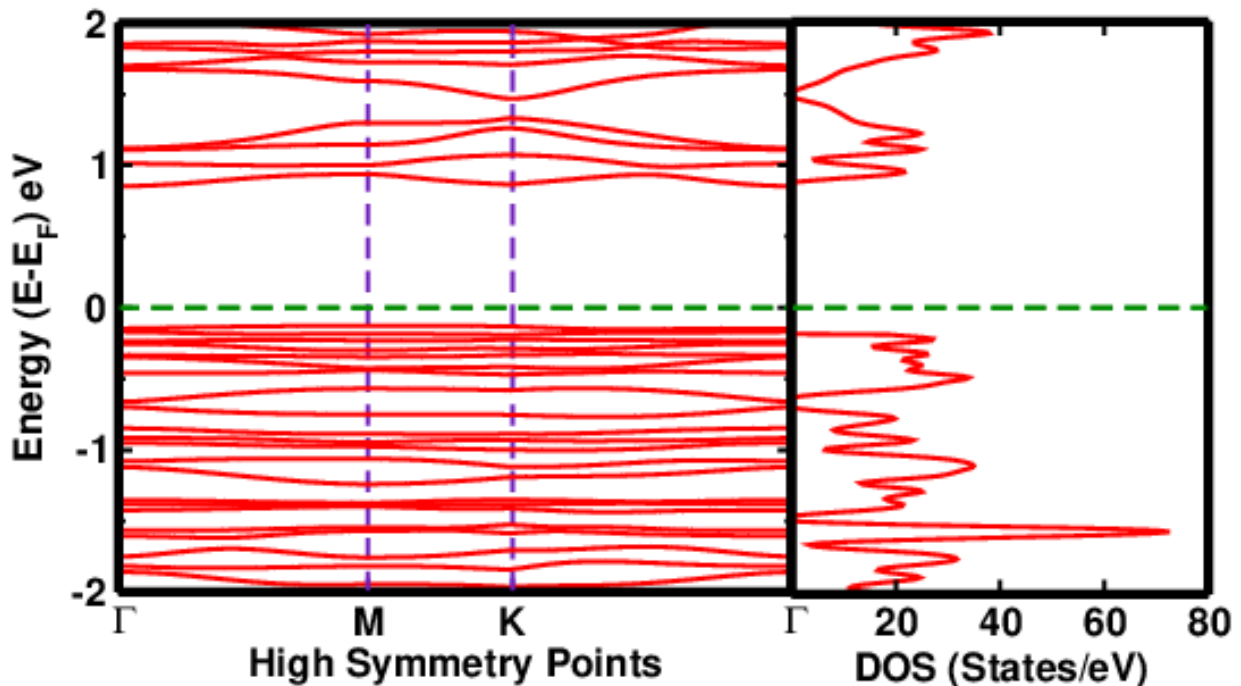
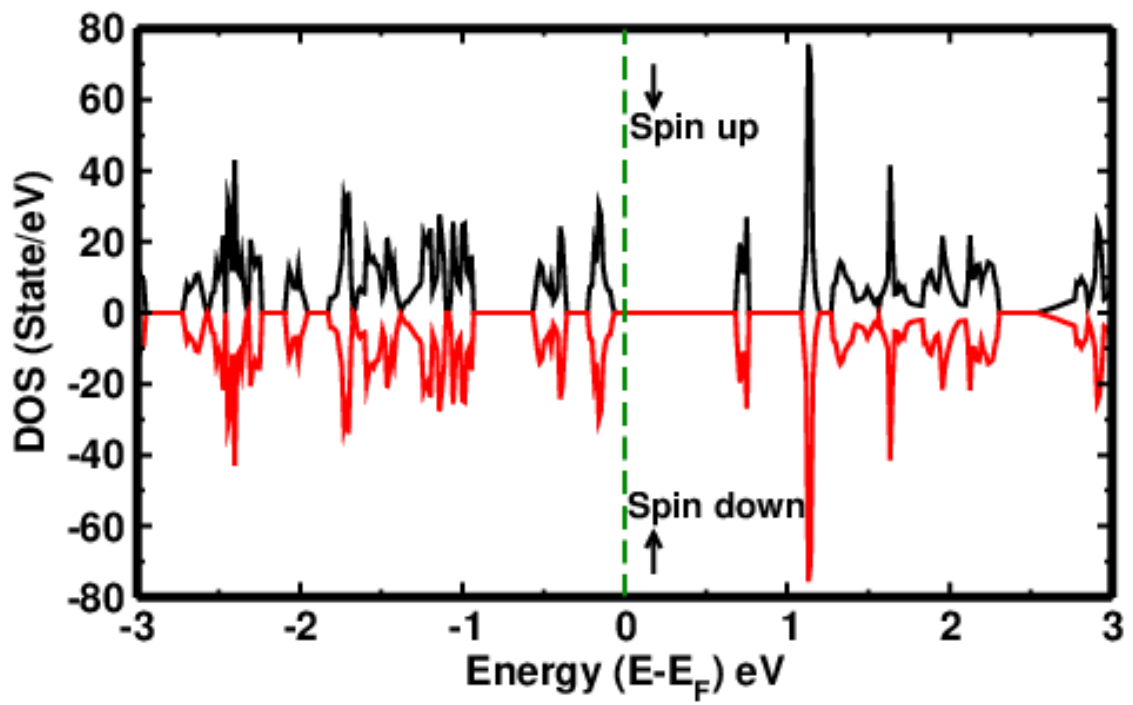


**Figure 4.11.** Band and DOS Plot of NO adsorbs Ni-Embedded Graphitic Carbon Nitride. where  $\Gamma$ -M-K- $\Gamma$  are high symmetry point, which is represented by a vertical dashed line. The horizontal dashed line represents Fermi level, which is set as 0 eV.

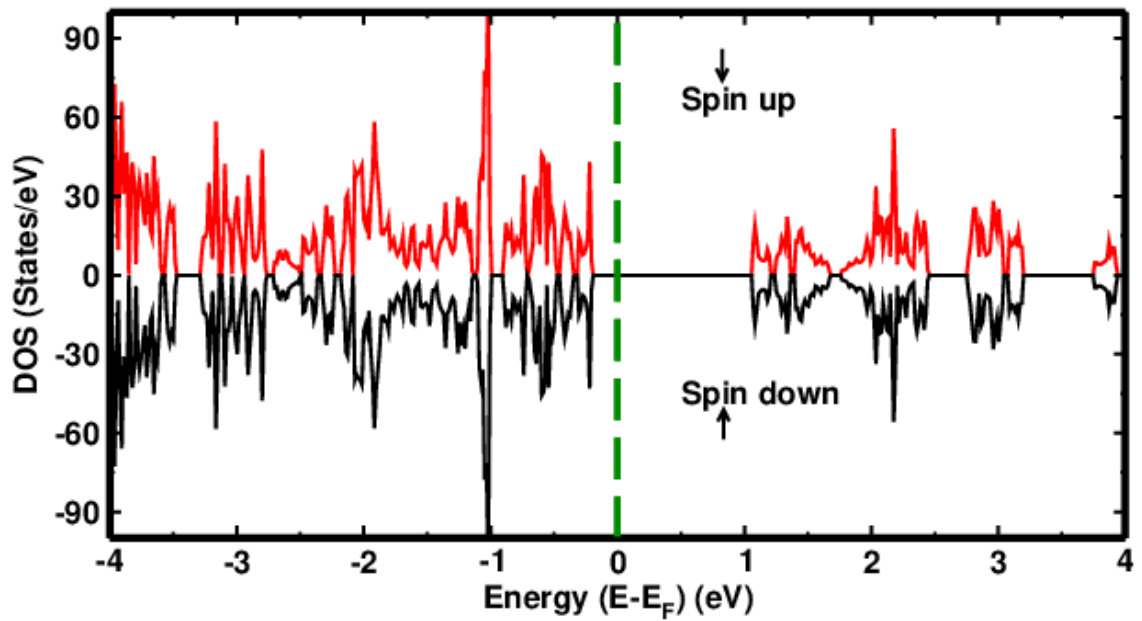
#### 4.5.2 Magnetic Properties of NO adsorbs Ni-Embedded Graphitic Carbon Nitride

In Figure 4.12b, and 4.12a, upper lines indicate DOS of spin up, and below lines indicate DOS of spin down of the Ni-Embedded GCN NO adsorbs Ni-Embedded GCN. Carefully observing this figure we can see that there are symmetry between spin up and spin down. The symmetry between spin up and spin down doesn't give the magnetic nature of the material. The magnetic moment of this material was found to be  $0.0 \mu_B$ . That means NO adsorbs Ni embedded GCN is not magnetic material.





(a)



(b)

**Figure 4.12.** (a) Magnetic Properties of Ni-Embedded Graphitic Carbon Nitride vertical dashed lines indicates Fermi energy level (b) Magnetic Properties of NO adsorbs Ni-Embedded Graphitic Carbon Nitride vertical dashed lines indicates Fermi energy level

## 4.6 NO adsorbs Pd-Embedded Graphitic Carbon Nitride

Pd is the transition metal that is embedded on the Graphitic Carbon Nitride. Simultaneously Nitric Oxide adsorbs on this Pd-Embedded Graphitic Carbon Nitride. Fig 4.13a (side view) and Fig4.13b (top view) are the structure of NO adsorbs Pd-Embedded Graphitic Carbon Nitride. The same relaxed structure is given in Fig 4.13c(side view) and Fig 4.13d (top view) respectively. Moreover, it can be found that with the adsorption of NO gas over Pd-Embedded GCN, the initial flat structure of pristine GCN automatically becomes wrinkle, because the buckle structure of GCN is more stable than the flat one, which is in agreement with the results [7]. Distance between respected atoms in Fig 4.13 is given in Appendix B. When comparing bond length with GCN and NO-GCN, the outer side of the bond length is about 3 Å longer whereas the inner side is unaffected.

The distance between Nitrogen and Oxygen in Nitric Oxide after relaxation was found to be 1.175 Å. Relaxation energy of the Nitric Oxide adsorbs Pd-Embedded GCN was found to be  $-492.28$  eV. Adsorption energy is calculated by the formula 2.6 and it is found to be  $-6.60$  eV. Here, chemisorption Nitric Oxide with Pd-Embedded GCN. Nitric Oxide forms the bond with the Palladium with bond length found to be 1.80 Å, which is greater than Pt-NO and Ni-NO.

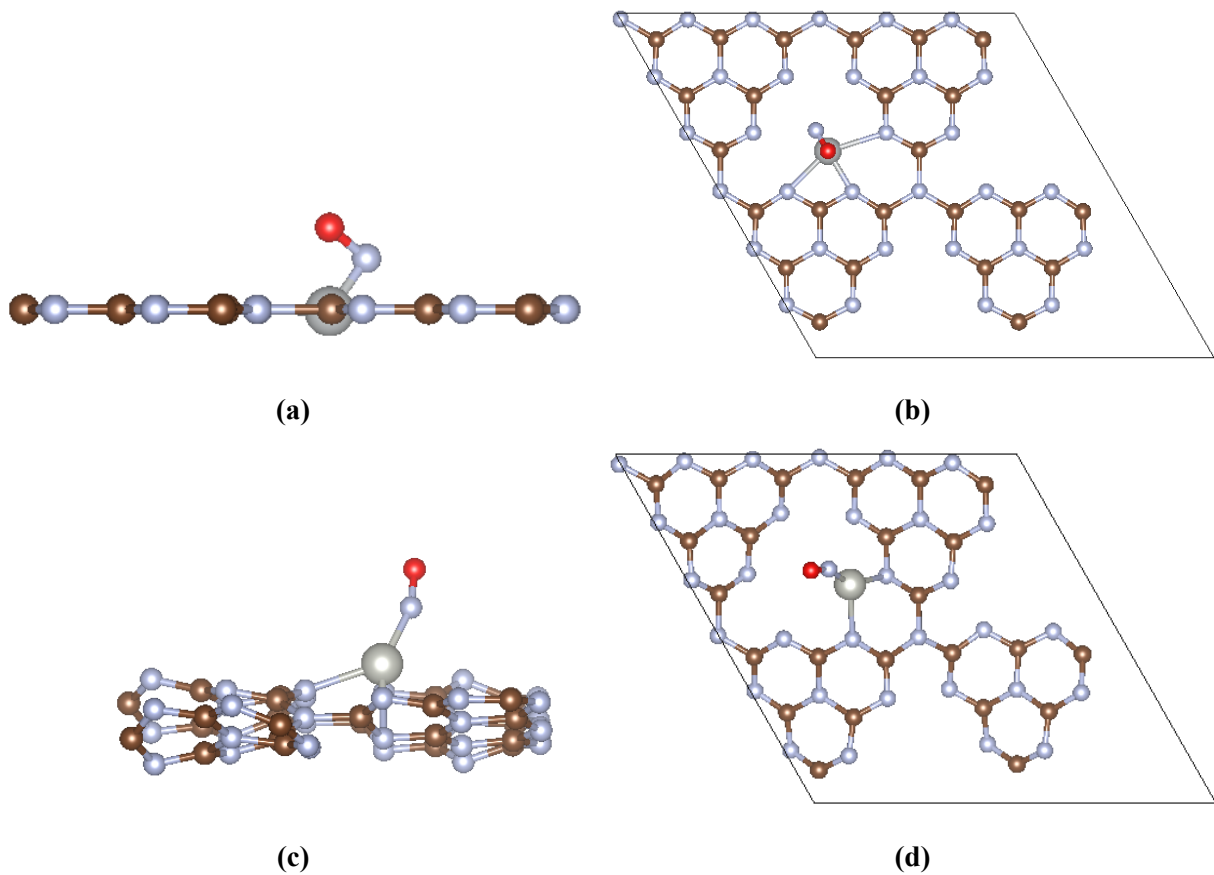


**Figure 4.13.** NO adsorbs Pd-Embedded Graphitic Carbon Nitride (a) side view of Pd-NO-GCN before relax (b) top view of Pd-NO-GCN before relax (c) side view of Pd-NO-GCN after relax (d) top view of Pd-NO-GCN after relax

#### 4.6.1 Electronic Properties of NO adsorbs Pd-Embedded Graphitic Carbon Nitride

Fig. 4.14, shows the band and DOS plot of NO adsorbs Pd-Embedded Graphitic Carbon Nitride. We found that the Fermi energy  $-0.65$  eV, which is comparable with the previous reports [11],[6], [28] and[29]. The results show that Pd-Embedded Graphitic Carbon Nitride with Nitric Oxide adsorbs, new energy states are introduced near the Fermi surface and modify the electronic properties of the system. It means the conductivity of the system is considerably increased. In Fig 4.14, some bands are added nearly on the Fermi surface so, the band gap of Pd-Embedded GCN becomes  $0.45$  eV. DOS is shifted towards the Fermi level, and the highest density of states is obtained at

energy level nearly  $-1$  eV (valence band), which is nearly equal to the 100 States/eV.

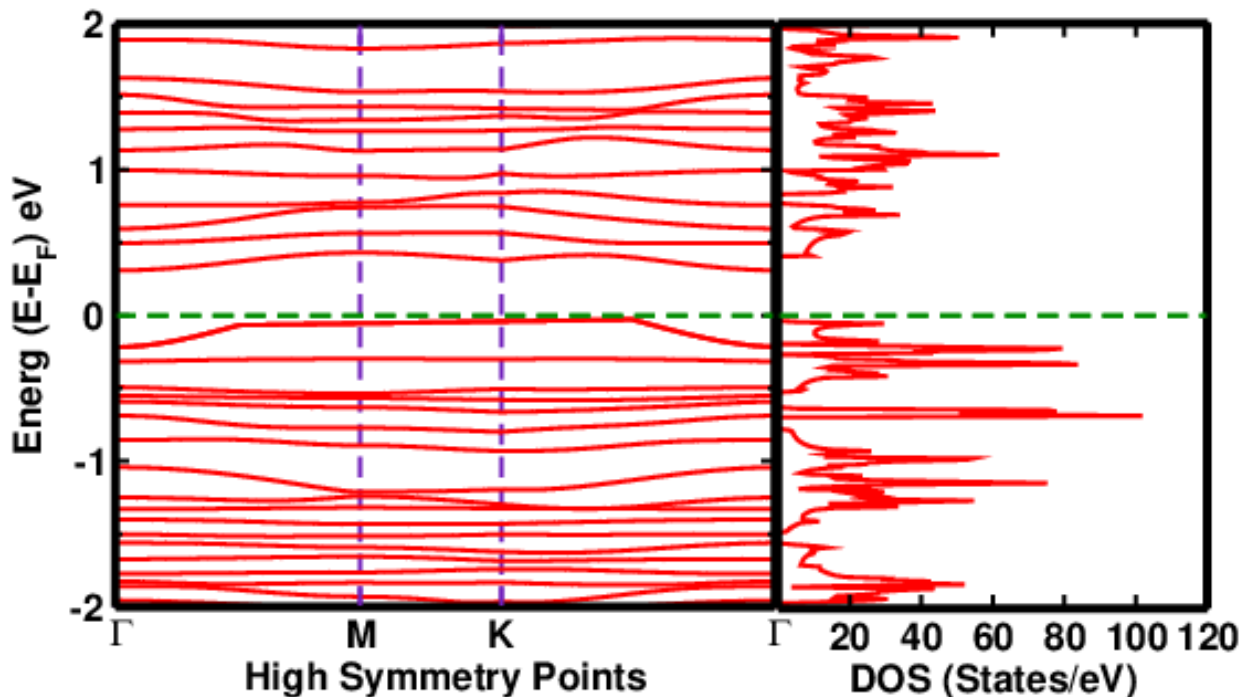
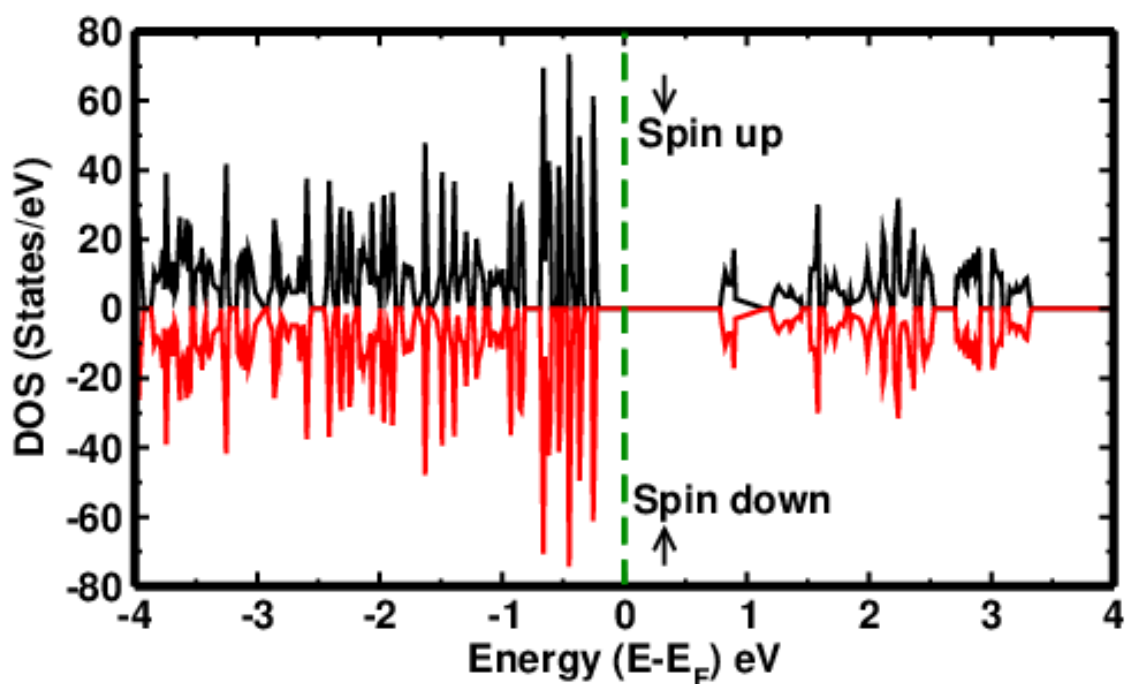


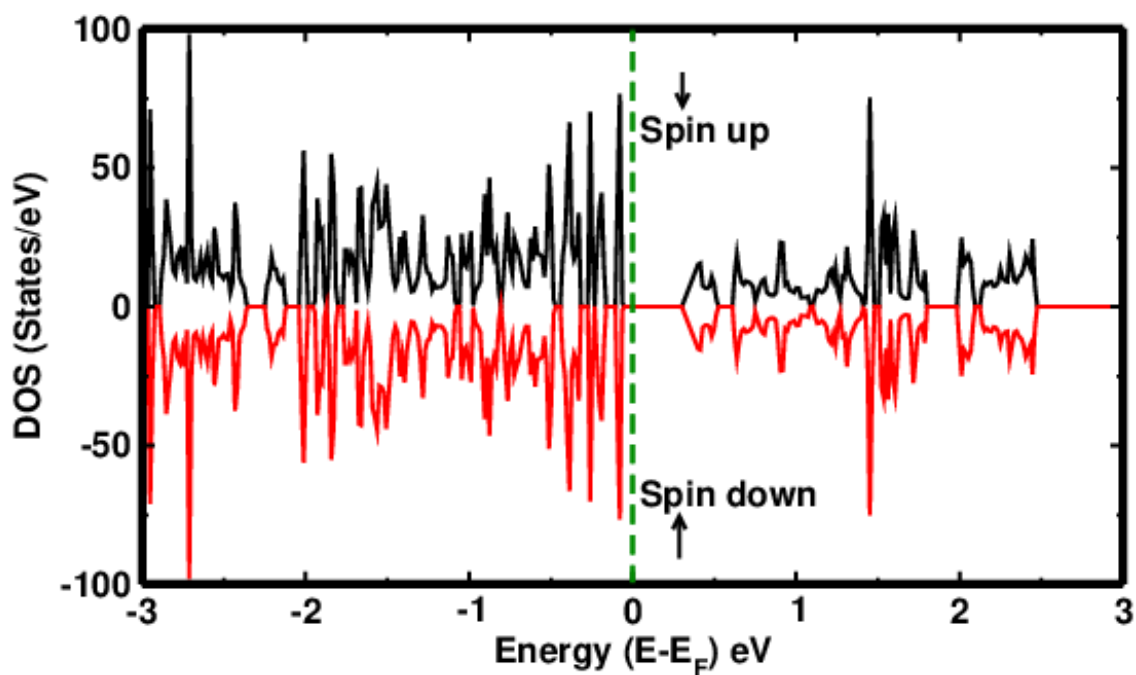
**Figure 4.14.** Electronic properties of NO adsorbs Pd-Embedded Graphitic Carbon Nitride. where  $\Gamma$ -M-K- $\Gamma$  are high symmetry point, which is represented by a vertical dashed line. The horizontal dashed line represents Fermi level, which is set as 0 eV.

#### 4.6.2 Magnetic Properties of NO adsorbs Pd-Embedded Graphitic Carbon Nitride

In Fig 4.15a and Fig 4.15b, upper lines indicate DOS of spin up, and below lines indicate DOS of spin-down of Pd-Embedded GCN and NO adsorbs Pd-Embedded GCN. Carefully observing these figures we can see that there is symmetry between spin up and spin down. The symmetry between spin up and spin down doesn't give the magnetic nature of the material. The magnetic moment of this material is found to be  $0.0 \mu_B$ . That means NO adsorbs Pd-Embedded GCN is not magnetic material.



(a)



(b)

**Figure 4.15.** (a) Magnetic Properties of Pd-Embedded Graphitic Carbon Nitride. The vertical dashed line indicates Fermi energy level. (b) Magnetic Properties of NO adsorbed Pd-Embedded Graphitic Carbon Nitride. The vertical dashed line indicates Fermi energy level.

## 4.7 NO adsorbs Pt-Embedded Graphitic Carbon Nitride

Platinum is the transition metal that is embedded on the Graphitic Carbon Nitride. Simultaneously Nitric Oxide adsorbs on this Pt-Embedded Graphitic Carbon Nitride. Fig 4.16a (side view) and Fig4.16b (top view) are the structure of NO adsorbs Pt-Embedded Graphitic Carbon Nitride. The same relaxed structure is given in Fig 4.16c (side view) and 4.16d (top view) respectively. Moreover, it can be found that with adsorption of NO gas over Pt-Embedded GCN, the initial flat structure of pristine GCN automatically becomes wrinkle, because the buckle structure of GCN is more stable than the flat one, which is in agreement with the previous results [7]. Distance between respected atoms in 4.16 is given in Appendix B. When comparing bond length with GCN and NO-GCN, the outer side of the bond length is about 3 Å longer whereas the inner side is unaffected.

The distance between nitrogen and oxygen in Nitric Oxide after relaxation was found to be 1.180 Å. Relaxation energy of the Nitric Oxide adsorbs Pt-Embedded GCN was found to be  $-493.2023$  eV. Adsorption energy is calculated by the formula 2.6 and it is found to be  $-8.74$  eV. Here, chemisorption of Nitric Oxide with Pt-Embedded GCN occurs. The bond length between Nitric Oxide and Platinum was found to be 1.74 Å, which is less than Pd-NO and greater than Ni-NO.

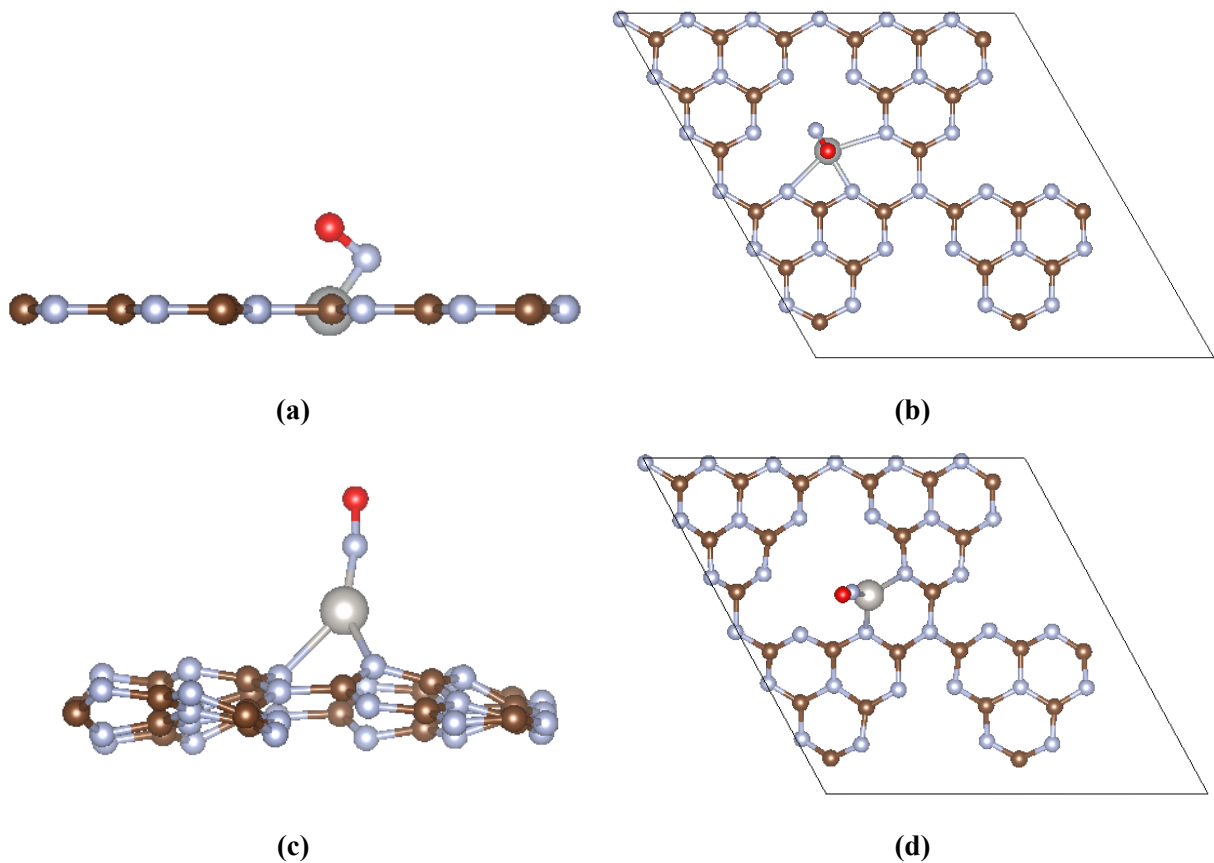


**Figure 4.16.** NO adsorbs Pt-Embedded Graphitic Carbon Nitride (a) side view of Pt-NO-GCN before relaxed (b) top view of Pt-NO-GCN before relaxed (c) side view of Pt-NO-GCN after relaxed (d) top view of Pt-NO-GCN after relaxed

#### 4.7.1 Electronic properties of NO adsorbs Pt-Embedded Graphitic Carbon Nitride

Fig. 4.17, shows the band and DOS plot of NO adsorbs Pt-Embedded Graphitic Carbon Nitride. We found that the Fermi energy  $-0.62$  eV, which is comparable with the previous results [11],[6], [29] and [28]. The results show that Pt embedded Graphitic Carbon Nitride with Nitric Oxide adsorbs, new energy states are introduced near the Fermi surface and modify the electronic properties of the system. It means the conductivity of the system is considerably increased. In Fig 4.17, some bands are added nearly on the Fermi surface so, the band gap of Pt-Embedded GCN becomes  $0.32$  eV. DOS is shifted towards the Fermi level, and the highest density of states is obtained at energy level

-1 eV (valence band), which is greater or equal to the 200 States/eV.

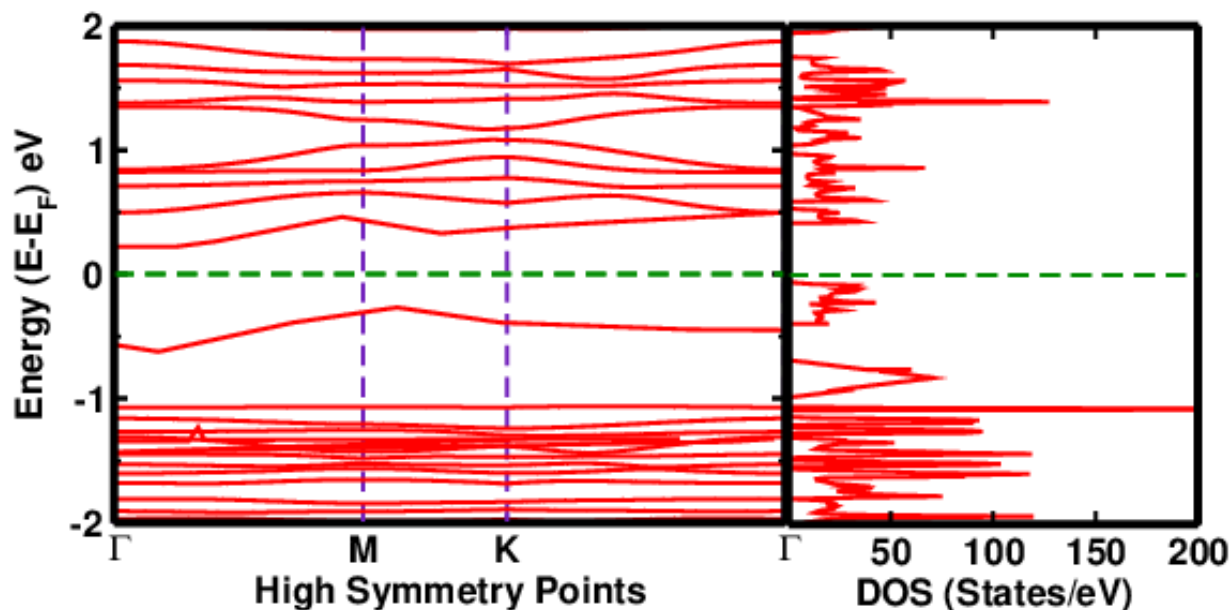


**Figure 4.17.** Electronic Properties of NO adsorbs Pt-Embedded Graphitic Carbon Nitride. Where  $\Gamma$ -M-K- $\Gamma$  are high symmetry point, which is represented by a vertical dashed line. The horizontal dashed line represents Fermi level, which is set as 0 eV.

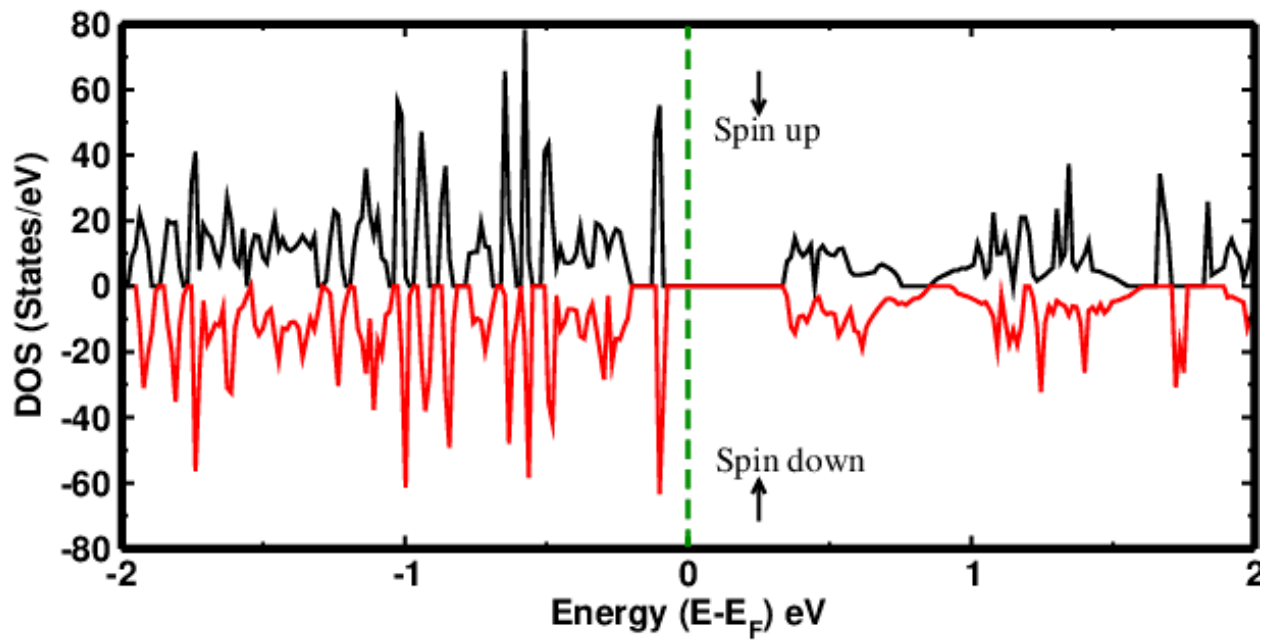
#### 4.7.2 Magnetic Properties of NO adsorbs Pt-Embedded Graphitic Carbon Nitride

Fig 4.18, shows that there is no symmetry in nature, so this material represents the magnetic property. Fig 4.24(a), shows the DOS plot of N atom in NO adsorbs Pt-Embedded Graphitic Carbon Nitride, where there is the symmetric distribution of spin up and spin down. So N atom doesn't give any magnetic moment. Fig 4.24(b) shows the DOS plot of C atom in NO adsorbs Pt-Embedded Graphitic Carbon Nitride, where there is the symmetric distribution of spin up and spin down. So C atom doesn't give any magnetic moment. Fig 4.24(c) shows the DOS plot of O atom in NO adsorbs Pt-Embedded Graphitic Carbon Nitride, where there is the symmetric distribution of spin up and spin down. So O atom doesn't give any magnetic moment.

But in Fig 4.2(d) there is no symmetric distribution between spin up and spin down so this atom



i.e. Platinum atoms gives the magnetic moment of this material which is found to be  $0.9816 \mu_B$ . This is due to the  $d_{xy}$  and  $d_{yz}$  orbital of the Platinum atom present in NO adsorbs Pt-Embedded GCN, which is shown in Fig 4.20.



**Figure 4.18.** DOS of NO adsorbs Pt-Embedded GCN with spin up and spin down directions.

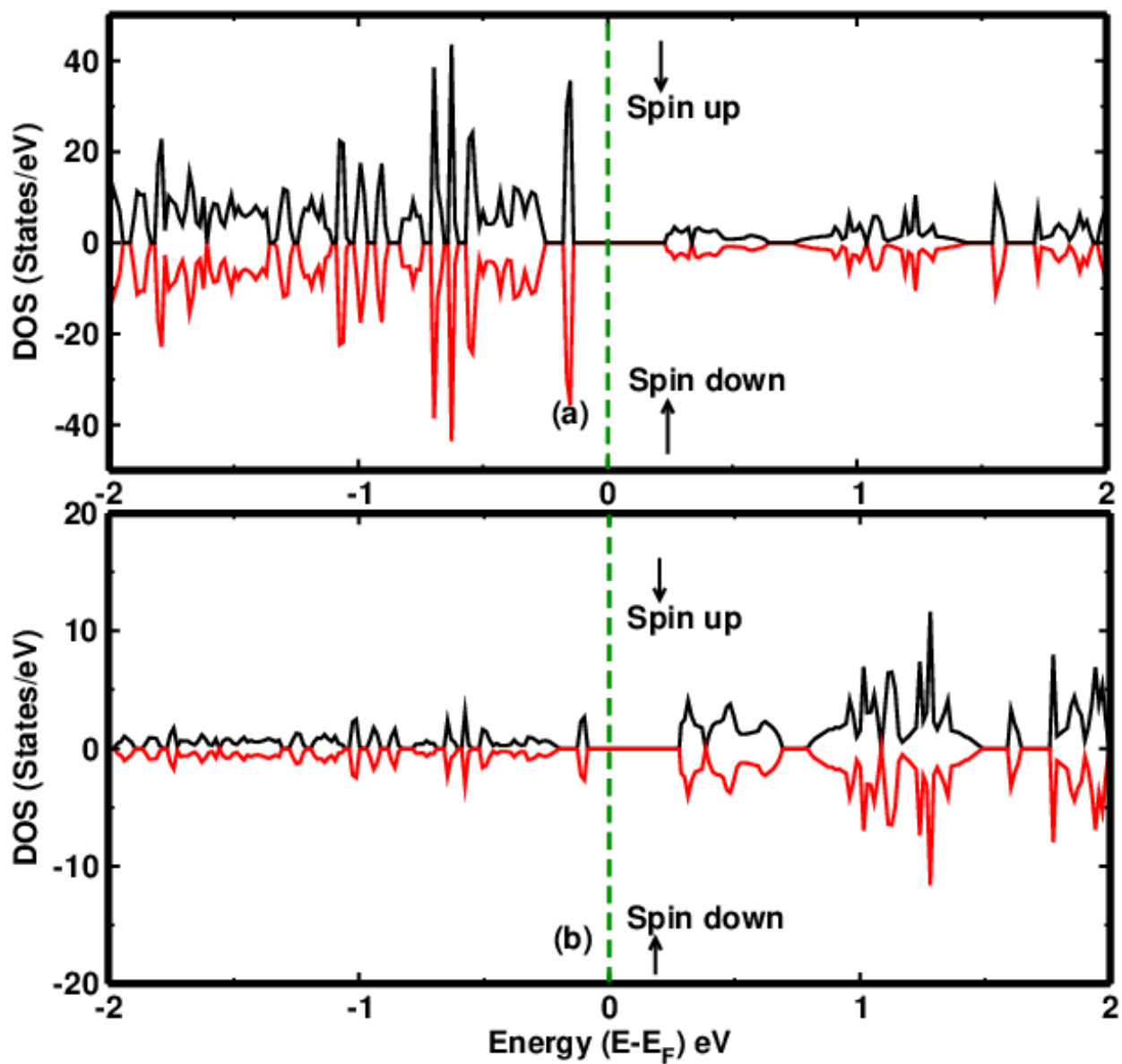


**Figure 4.19.** PDOS of NO adsorbs Pt-Embedded GCN with spin up and spin down directions. (a)PDOS of N atom with spin up and spin down in NO adsorbs Pt embedded GCN. (b)PDOS of C atom with spin up and spin down in NO adsorbs Pt embedded GCN.

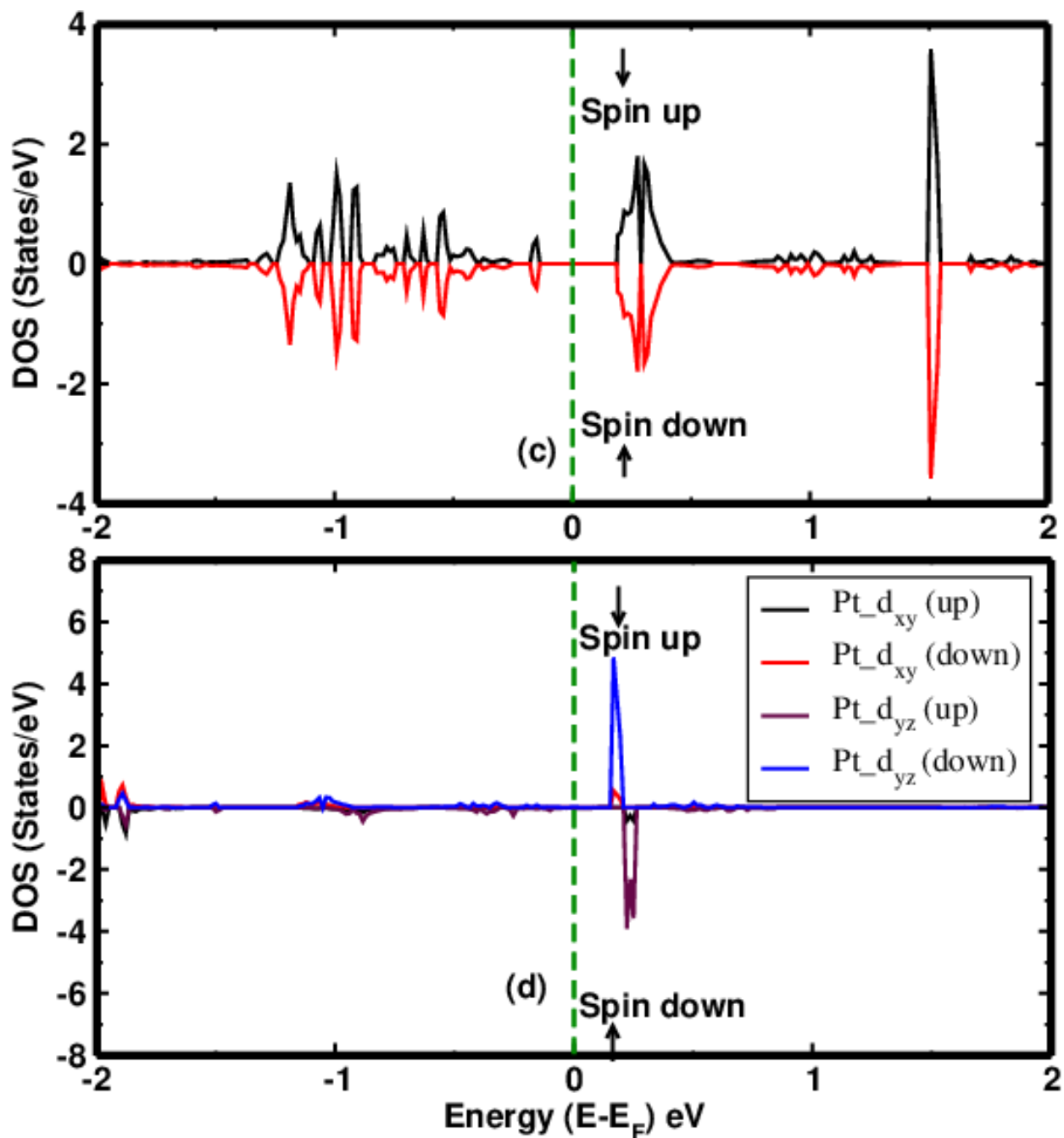


**Figure 4.20.** DOS of NO adsorbs Pt-Embedded GCN with spin up and spin down directions. (c)DOS of O atom with spin up and spin down in NO adsorbs Pt-Embedded GCN. (d)DOS of Pt atom with spin up and spin down with  $d_{xy}$  and  $d_{yz}$  orbital in NO adsorbs Pt-Embedded GCN.

# Chapter 5

## Conclusion and Future Prospects

### 5.1 Conclusion

The functionalization of transition metal-embedded Graphitic Carbon Nitride by the adsorption of NO to its the surface has been investigated computationally by using first principles density functional theory. The aim of this calculation is to compare the adsorption behavior of NO on Ni, Pd, Pt embedded Graphitic Carbon Nitride. Projector Augmented Wave (PAW) pseudopotential with Perdew-Burke-Ernzerhof (PBE) exchange-correlation functional in the Generalized Gradient Approximation (GGA) was used for self-consistent, electronic and magnetic calculations. The crystal structure was first optimized to get the relaxed structure of a single GCN and optimized  $2 \times 2$  supercell with a k point grid of  $5 \times 5 \times 1$ . Kinetic energy cutoff 550 eV, was set up for plane-wave basis set expansion and limiting the total number of plane waves in calculations. We use the ‘Gaussian’ type of smearing with smearing width 0.005 eV. And this smearing type was changed to ‘tetrahedron’ for the band and DOS calculation. After relaxing the structure, SCF calculation was performed for GCN, NO adsorbs GCN, NO adsorbs Ni embedded GCN, NO adsorbs Pd embedded GCN and NO adsorbs Pt embedded GCN.

The adsorption energy of Nitric Oxide on Graphitic Carbon Nitride is found to be  $-1.68$  eV. The adsorption energy of Nitric Oxide on Ni, Pd, Pt-Embedded Graphitic Carbon Nitride is  $-8.63$  eV,  $-6.61$  eV and  $-8.74$  eV respectively. This shows that Pt-Embedded Graphitic Carbon Nitride is

more negative i.e more absorbance energy other than Ni, and Pd.

The main findings of our research are sum as follows.

- The structure of the NO adsorbs Ni, Pd, and Pt-Embedded GCN becomes a buckled structure.
- Fermi energy of the GCN, NO adsorbs on GCN, NO adsorbs on Ni, Pd, Pt-Embedded GCN are  $-1.72$  eV,  $-1.36$  eV,  $-0.65$  eV,  $-0.64$  eV and  $-0.61$  eV respectively.
- Band gap of the GCN, NO adsorbs on GCN, NO adsorbs on Ni, Pd, Pt-Embedded GCN are  $1.3$  eV,  $1.12$  eV,  $0.98$  eV,  $0.45$  eV, and  $0.32$  eV respectively.
- Magnetic moment of the GCN, NO adsorbs on GCN, NO adsorbs on Ni, Pd, Pt-Embedded GCN are  $0.0 \mu_B$ ,  $0.0 \mu_B$ ,  $0.0 \mu_B$ ,  $0.0 \mu_B$ , and  $0.98 \mu_B$  respectively.

## 5.2 Future Prospectus

In this study, we study the adsorption behavior of Nitric Oxide (NO) molecules over Ni, Pd, and Pt-Embedded Graphitic Carbon Nitride (GCN). While performing our research work, we felt that for this molecule there are still many areas in which the researcher will have interested in the study.

In this regard, the following works have been strongly recommended for a future prospectus.

1. The study will be performed by taking different functional such as SCAN, PBE sol, B3LYP, etc.
2. The study will be performed by using the bilayer structure of Graphitic Carbon Nitride.
3. Optical and mechanical properties of Nitric Oxide adsorbs over Ni, Pd, Pt-Embedded Graphitic Carbon Nitride will be studied.
4. The study will be performed for  $3 \times 3$ ,  $4 \times 4$ ,  $5 \times 5$  Graphitic Carbon Nitride supercell.

# References

- [1] B. S. Bahal, G. D. Tauli, and A. Bahl, *Essentials of physical chemistry* (26<sup>th</sup>ed.), India, S.Chand & Company Ltd.
- [2] R. S. Chouhan, I. Jerman, D. Heath, S. Bohm, S. Gandhi, V. Sadhu, S. Baker, and M. Horvat, *Nano select* **2**, 712 (2021).
- [3] Y. Wang, L. Liu, T. Ma, Y. Zhang, and H. Huang, *Adv. Funct. Mater* **31**, 2102540 (2021).
- [4] <https://www.britannica.com/science/transition-metal> (viewed at 08/12/2022)
- [5] H. Basharnavaz, A. H. Yangjeh, and M. Mousavi, *Appl. Surf. Sci* **456**, 882 (2018).
- [6] H. Basharnavaz, A. H. Yanngjeh, and S. H. Kamali, *Phys. Lett. A* **383**, 2472 (2019).
- [7] H. Basharnavaz, A. H. Yangjeh, and S. H. Kamali, *Mater. Chem. Phys* **231**, 264 (2019).
- [8] D. Ghosh, G. Periyasamy, B. Pandey, and S. k. Pati, *J. Mater. Chem. C* **2**, 7943 (2014).
- [9] S. M. Aspera, M. David, and H. Kasai, *JJAP* **49**, 115703 (2010).
- [10] A. M. Hu, H. J. Luo, and W. Z. Xiao, *J. Magn. Magn. Mater* **493**, 165745 (2020).
- [11] Y. xu, S. X. Jiang, W. J. Sheng, L. x. Wu, G. Z. Nie and Z. Ao, *Appl. Surf. Sci.* **501**, 144199 (2020)
- [12] H. Z. Wu, L. M. Liu, and S. J. Zhao, *Appl. Surf. Sci* **358**, 363 (2015).
- [13] S. M. Aspera, H. Kasai, and H. Kawai, *Surf Sci* **606**, 892 (2012).
- [14] M. Born, J. R. Oppenheimer, *Ann. Physik* **84**, 457 (1927)

- [15] E. Kaxiras, *Atomic and Electronics Structure of Solids*, (1<sup>st</sup> ed.), New York, Cambridge University Press.
- [16] B. K. Agrawal, H. Prakash, *Quantum Mechanics*, (12<sup>th</sup> printing), India, PHI Learning Private Limited
- [17] P. Hohenberg and W. Kohn, Phys. Rev. **136**, B864 (1964).
- [18] W. Kohn and L. J. Sham, Phys. Rev. **140**, A1133 (1965).
- [19] J. P. Perdew, K. Burke, M. Ernzerhof, Phys. Rev. **78**, 1396 (1997)
- [20] B. P. Poudel, N. Pantha and N. P. Adhikari, NepJOL **3**, 24 (2015)
- [21] <https://www.vasp.at/info/about/> (viewed at 08/11/2022)
- [22] [https://www.vasp.at/wiki/images8/8e/VASP\\_elec\\_min\\_flowchart.png](https://www.vasp.at/wiki/images8/8e/VASP_elec_min_flowchart.png) (viewed at 08/11/2022)
- [23] <https://www.vasp.at/py4vasp/latest/> (viewed at 08/12/2022)
- [24] <http://www.jp-minerals.org/vesta/en/> (viewed at 2/11/2022)
- [25] V. Wang, N. Xu, Jin-Cheng Liu, Gang Tang and Wen-Tong Geng, Comput. Phys. Commun. **267**, 108033 (2021).
- [26] <http://www.p4vasp.at/> (viewed at 12/11/2022)
- [27] <https://pubchem.ncbi.nlm.nih.gov/compound/nitric-oxide> (viewed at 2/11/2022)
- [28] F. Fina, S. K. Callear, G. M. Carins, and J. T. S. Irvine, Chem. Mater. **27**, 2612 (2015)
- [29] M. Fronczak, J. Environ. Chem. Eng. **8**, 104411 (2020).
- [30] G. Imanzadeh, H. Basharnavaz, A. H. Yangjeh, and S. H. Kamali, Mater. Chem. Phys **252**, 123117 (2020).
- [31] F. Safdari, A. N. Shamkhali, M. Tafazzoli, and G. Parsafar, J Mol Liq. **260**, 423 (2018).

# Appendices

## Appendix A

### Input File Information

#### A.1 Relax Calculation INCAR Input File

```
#RELAXATION
SYSTEM = GCN
ISTART = 0 # NEW CALCULATION
ICHARGE = 2
#ELECTRONIC OPTIMIZATION
PREC = ACCURATE # 1.3 OF THE ENMAX IN THE POTCAR
ENCUT = 550
ISMEAR = 0
SIGMA = 0.05
EDIFF = 1E-07
NELM = 100
LREAL = .FALSE.
#IONIC RELAXATION
EDIFFG = -1E-02
NSW = 200
ISIF = 3 # RELAXING ATOMS, CELL, SHAPE, AND CELL VOLUME
IBRION = 2
```



NCORE = 2

## **A.2 SCF Calculation INCAR Input File**

```
#SCF
SYSTEM = GCN
ISTART = 0 # NEW CALCULATION
ICHARGE = 2
# ELECTRONIC OPTIMIZATION
PREC = ACCURATE
ENCUT = 550
ISMEAR = 0
SIGMA = 0.05
EDIFF = 1E-07
NELM = 100
LREAL = .FALSE.
# IONIC RELAXATION
EDIFFG = -1E-02
NSW = 0 # NUMBER OF IONIC STEPS
IBRION = -1 # IONS ARE NOT MOVED
NCORE = 2
ISYM = 0
LWAVE = .FALSE.
LCHARGE = .TRUE.
```

## **A.3 DOS and Band Calculation INCAR Input File**

```
#DOS AND BAND CALCULATION
SYSTEM = GCN
PREC = ACCURATE
ISTART = 1 # CHARGE DENSITIES READ FROM CHGCAR
```

```
ICHARGE = 11 # TO OBTAIN EIGEN VALUES
# ELECTRONIC OPTIMIZATION
ENCUT    = 550
ISMEAR   = -5          # TETRAHEDRON METHOD
#DOS
LORBIT   = 11 # OUTPUT DOSCAR AND PROCAR
NEDOS    = 1000
EMIN     = -5
EMAX     = 5
SIGMA    = 0.05
EDIFF    = 1E-07
NELM     = 100
LREAL    = .FALSE.
# IONIC RELAXATION
EDIFFG   = -1E-02
NSW      = 0
IBRION   = -1      # IONS ARE NOT MOVED
NCORE    = 2
ISYM     = 0
LWAVE    = .FALSE.
LCHARGE  = .TRUE.
```

## Appendix B

### B.1 Bond Length

Table 5.1. Bond length

Bonds	Bonds length(Å)				
	GCN	NO-GCN	Ni-NO-GCN	Pd-NO-GCN	Pt-NO-GCN
C2-N3	1.47	1.41	1.45	1.44	1.44
N3-C9	1.47	1.43	1.41	1.42	1.43
C9-N13	1.33	1.33	1.34	1.35	1.34
N13-C5	1.33	1.33	1.31	1.33	1.32
C5-N9	1.33	1.33	1.34	1.34	1.34
N9-C13	1.33	1.34	1.37	1.37	1.38
C13-N21	1.33	1.34	1.32	1.33	1.33
N21-C21	1.33	1.32	1.34	1.33	1.33
C21-N5	1.39	1.39	1.43	1.40	1.43
N5-C5	1.39	1.39	1.38	1.40	1.39
N5-C17	1.39	1.40	1.42	1.34	1.39
C17-N29	1.33	1.34	1.33	1.34	1.34
N29-C9	1.33	1.34	1.33	1.31	1.34
C17-N17	1.33	1.34	1.31	1.33	1.34
N17-C1	1.33	1.34	1.34	1.35	1.34
C1-N25	1.33	1.33	1.34	1.33	1.34
N1-C11	1.47	1.45	1.44	1.43	1.46
C11-N15	1.33	1.33	1.37	1.34	1.32
N15-C7	1.33	1.33	1.33	1.33	1.32
C7-N11	1.33	1.33	1.36	1.34	1.33
N11-C15	1.33	1.34	1.34	1.34	1.34
C15-N23	1.33	1.33	1.34	1.35	1.34
N23-C23	1.33	1.33	1.33	1.34	1.33

C23-N7	1.39	1.40	1.40	1.39	1.39
N7-C7	1.39	1.39	1.40	1.40	1.39
N7-C19	1.39	1.40	1.40	1.40	1.40
C19-N19	1.33	1.33	1.34	1.33	1.33
N19-C3	1.33	1.34	1.34	1.35	1.33
C3-N27	1.33	1.34	1.34	1.34	1.34
N27-C23	1.33	1.32	1.34	1.34	1.44
N4-C10	1.47	1.45	1.45	1.43	1.43
C10-N14	1.33	1.34	1.32	1.33	1.32
N14-C6	1.33	1.34	1.32	1.32	1.32
C6-N10	1.33	1.33	1.33	1.32	1.31
N10-C14	1.33	1.34	1.33	1.33	1.32
C14-N22	1.33	1.34	1.35	1.35	1.35
N22-C22	1.33	1.32	1.35	1.34	1.34
C22-N6	1.39	1.39	1.40	1.40	1.40
N6-C6	1.39	1.40	1.39	1.39	1.38
N6-C18	1.39	1.39	1.40	1.40	1.40
C18-N30	1.33	1.34	1.37	1.34	1.34
N30-C10	1.33	1.33	1.34	1.34	1.42
C14-N2	1.47	1.40	1.44	1.44	1.41
N2-C12	1.47	1.45	1.43	1.43	1.41
C12-N16	1.33	1.32	1.34	1.33	1.32
N16-C8	1.33	1.34	1.35	1.33	1.33
N12-C16	1.33	1.34	1.36	1.34	1.34
C16-N24	1.33	1.34	1.32	1.34	1.34
N24-C24	1.33	1.33	1.31	1.32	1.32
C24-N8	1.39	1.40	1.41	1.41	1.40
N8-C8	1.39	1.39	1.40	1.41	1.40
N8-C20	1.39	1.39	1.37	1.38	1.37
C20-N32	1.33	1.34	1.32	1.32	1.32

N32-C12	1.33	1.34	1.35	1.34	1.35
C24-N28	1.33	1.33	1.33	1.33	1.31
N28-C4	1.33	1.32	1.32	1.32	1.30
C4-N20	1.33	1.34	1.37	1.36	1.37